remote sensing

MDPI

Review

From Its Core to the Niche: Insights from GPR Applications

Federico Lombardi [1,*], Frank Podd [2] and Mercedes Solla [3]

[1] Department of Civil and Environmental Engineering, Politecnico di Milano, Piazza Leonardo da Vinci 32, 20133 Milan, Italy
[2] Department of Electrical & Electronics Engineering, The University of Manchester, Oxford Road, Manchester M13 9PL, UK; frank.podd@manchester.ac.uk
[3] CINTECX, GeoTECH Research Group, Universidade de Vigo, 36310 Vigo, Spain; merchisolla@uvigo.es
* Correspondence: federico.lombardi@polimi.it

Abstract: Thanks to its non-destructive, high-resolution imaging possibilities and its sensitivity to both conductive and dielectric subsurface structures, Ground-Penetrating Radar (GPR) has become a widely recognized near-surface geophysical tool, routinely adopted in a wide variety of disciplines. Since its first development almost 100 years ago, the domain in which the methodology has been successfully deployed has significantly expanded from ice sounding and environmental studies to precision agriculture and infrastructure monitoring. While such expansion has been clearly supported by the evolution of technology and electronics, the operating principles have always secured GPR a predominant position among alternative inspection approaches. The aim of this contribution is to provide a large-scale survey of the current areas where GPR has emerged as a valuable prospection methodology, highlighting the reasons for such prominence and, at the same time, to suggest where and how it could be enhanced even more.

Keywords: Ground-Penetrating Radar; NDT; near surface geophysics; applications of GPR

Citation: Lombardi, F.; Podd, F.; Solla, M. From Its Core to the Niche: Insights from GPR Applications. *Remote Sens.* **2022**, *14*, 3033. https://doi.org/10.3390/rs14133033

Academic Editor: Roberto Orosei

Received: 5 May 2022
Accepted: 20 June 2022
Published: 24 June 2022

1. Introduction

The plethora of GPR applications is growing rapidly, since GPR is now capable of producing high-resolution, 3D volume images of the shallow subsurface, which is rare in other non-destructive methodologies. In addition, being a reflection methodology, it allows for the joint measurement of both the geophysical and geometrical features of the problem, thus providing information on both the subsurface stratigraphy and the characteristics of the encountered material. This double potential has secured the technique a favorable place within a large number of domains, spanning from applications within the engineering and infrastructure inspection fields, possibly representing the core research domains, to the exploration for natural resources and geology.

Historically, the development of the GPR methodology has followed the invention of radar, and in 1910, only six years after Hülsmeyer obtained the first patent for his naval anti-collision system (patent DE 165546), Leimbach and Löwy applied for a patent to implement such technology to locate buried objects (patent DE 237944). The approach consisted of inserting a pair of transmitter and receiver antennas into an array of vertical boreholes and then correlating the recorded signal magnitude with the value obtained when successive pairs were used. In addition, they also suggested that the use of surface-laid antennas could lead to the determination of reflections from ground water interfaces. The first pulse radar system for geotechnical applications was introduced by Hülsenbeck in 1926 (patent DE 489 434), who developed a technology that is still widely used after almost a century, and who also highlighted that signal reflections are generated by any dielectric variations, not only when conductivity differences occur. Except for some early experiments aimed at measuring the depth of glaciers in 1929 [1], a campaign widely acknowledged to represent the world's first GPR survey, the technology was largely overlooked until late 1950s, when

eight US Air Force planes attempting to land in Greenland crashed because the onboard radar systems were actually seeing through the ice and therefore provided the pilots with an erroneous altitude measurement (Lost Squadron, 1942 [2]). This accidental event is considered the spark of the understanding of the potential of the radar methodology for exploring the subsurface and sounding geological materials. The earliest consequence was the inclusion of radar equipment onboard the Apollo 17, the Apollo Lunar Sounder Experiment (1972 [3]), with the aim of studying the moon's surface and subsurface.

Since the mid-1960s, the GPR technique was mainly researched for military applications as a tunnel-detection technology, in particular during the Vietnam War [4] and for locating tunnels under the demilitarized zone separating North and South Korea [5]. The first commercially available GPR devices appeared during the 1970s. From then on, industrial players, such as public utility and construction companies, became interested in such subsurface investigation tools, regarded as a fast and effective means for utility mapping under city streets [6]. Additionally, GPR became a publicly recognized instrument for supporting forensic investigations after the well-known "Fred West murders" case (1994 [7]), where it was able to accurately locate the remains of a number of victims buried under a concrete basement [8]. Since then, thanks to ever-increasing signal recovery and analysis techniques, hardware design, and instrumentation developments, the last decades have witnessed the evolution of GPR from a simple locator method to a quasi-quantitative subsurface interpretative tool.

Typically, GPR systems consist of separate transmitter and receiver antennas, even if they are housed in a single case with no means of varying the antenna geometry, commonly referred to as the quasi-monostatic configuration. An additional distinction is made depending on whether the equipment is working in contact with the surface (ground coupled) or above it (air launched), though the exact height at which antennas need to be placed for the configuration to be considered air launched is poorly defined, as well as how close is close enough to be considered ground coupled. The choice of one or the other approach represents a trade-off between operational suitability, data quality, and interpretability [9].

Considering that the probability of detection degrades rapidly as the sensor is lifted from the ground and that surface topography could severely affect the quality of the received data, ground-coupled GPR measurements are generally more effective. Reasons for this are the effect of the surface topography and roughness, which will randomly scatter the incident GPR wave, thus making the received data difficult to analyze and complicating the prediction of the effective propagating waveform, and the degraded coupling efficiency, since complex angles of refraction might occur. In addition, it should be noted the increased distance to the buried object. However, working with an air-launched configuration has its clear advantages, especially considering that it can be operated at higher speeds and is more suitable to vehicle mountings, thus allowing larger areas to be surveyed. Signal penetration and data resolution are highly enhanced through the use of a ground-coupled platform, as it is less prone to external noise and surface clutter and benefits from a theoretically perfect coupling between the antennas and the soil interface. In addition, the propagating waveform remains almost unaffected by the previously mentioned phenomena and, in principle, is closely similar to the emitted one, hence it can be used to more intuitively predict and interpret data [10–12]. Nevertheless, ground-coupled systems survey an area at slower speeds and cannot be operated on every surface topography.

Following these considerations, it is clear that air-launched configurations are the method of choice when there is the need for surveying large areas (such as transport infrastructures, bridges, and dams, as well as archeological and agricultural applications) and/or when the target of interest does not exhibit significant geometry variations (as is the case of geological horizons and environmental stratigraphy delineation). Finally, detaching the system from the surface is necessary when the roughness of the ground is relevant or when the contact might represent a safety concern, such as for security and demining operations. On the other hand, when deeper aspects are to be evaluated with high spatial resolution, a ground-coupled approach can by far surpass its counterpart. In particular, building

material characterization, including cracking and debonding, structures inspections, and cultural heritage condition, but also forensic studies and contaminant detection, are just few examples of applications where a ground-coupled approach is preferably.

Given these considerations, the aim of this contribution is to provide a comprehensive review of the major application areas in which GPR is currently being adopted, defining for each of them the specific research question that is addressed and detailing why the GPR technique has proven to be a valuable tool.

This review starts with civil engineering applications, in which GPR has played and is still playing a pivotal role for its non-destructive operations and high sensitivity to metallic objects. The contribution then explores another fundamental research topic of the technique, i.e., cultural heritage diagnosis and monitoring, one of the domains that has greatly benefited from the widespread adoption of GPR. Forensic and security applications represent two contexts in which GPR has already proven its value, but also where it is still confined at a marginal level, hindered by the strong need of human experience and interpretation, as for buried graves or search-and-rescue tasks, and by the expensive nature of the technology, particularly for the humanitarian assistance context.

The use of GPR for environmental investigations embraces both established applications, focusing on subsurface characterization and monitoring in both land and glacial scenarios, as well as emerging topics, including surface mining surveys.

Finally, this paper reviews the challenges and opportunities for GPR in the domain of geology. This application area includes sedimentary structure reconstruction for stratigraphic studies and fractures mapping, and freshwater investigations, where the objectives of the study go beyond the plain geometrical profiling of the underwater boundary.

2. GPR Applications in Civil Engineering

GPR is considered one of the most efficient, easy to operate, least traffic disrupting, and multi-application NDT in civil engineering applications [13]. Most of the GPR developments focus on detecting rebar and other linear metal targets (e.g., tendon ducts), and hidden utilities, both metal and non-metal, such as pipes and cables. The detection of hidden utilities is crucial prior to other invasive works such as excavation. The main findings of GPR within this application field are piping distribution and dimensioning, identification of utility material type, fluid/void ratio in case of non-metal pipes, leakage detection, rebar configuration and dimensioning, and corrosion [14–16].

GPR has also been widely used for transport infrastructure inspection, including the evaluation of roads, highways, and runways, as well as railways. Within this framework, the use of air-coupled systems mounted on mobile vehicles allows for the evaluation of in-service pavements without major disturbance to users, which means data collection can occur at high speeds, continuously, and in non-contact mode. Regarding road-pavement assessment (flexible and rigid), GPR provides valuable information in measuring thicknesses, aiming to identify deficiencies that compromise the proper behavior of pavements, and in detecting subsurface distresses (cracking, debonding and delamination, subsidence, and cavities) [17,18]. However, the effectiveness of the method in determining layer thickness and damages is affected by the presence of water, the high iron content in the aggregates, and metal presence (e.g., vehicles) in urban environments. Moreover, for an optimal determination of layer thickness, the system needs a calibration process (e.g., coring, using a metal plate, with the common-mid-point (CMP) method). On the other hand, the detection of cracks depends on the frequency antenna used, higher frequencies provided higher resolution, the geometry of the crack (width, depth, and orientation), and its condition (filled with foreign material, filled with bitumen, filled with water, empty, etc.) [19]. Other aspects that can be investigated with the GPR method are material density, porosity, moisture content, and subgrade condition [20,21]. For the latter, the most important limitation is the signal attenuation due to the high content of clay and water in this section of the pavement structure. In the case of rigid pavements, GPR is widely used to map rebar, cover depth to the rebar, and measure damages such as corrosion and delamination [22,23]. The main

applications in ballast-condition assessment consist of measuring ballast-layer thickness, detecting settlements, and analyzing fouling and moisture content [24–26]. In railways inspections, the main limitation is the presence of steel sleepers and rails that can result in a constant reflection, masking the deeper information.

For tunneling inspections, GPR applications comprehend thickness measurements in concrete segments and grouting and undertake the detection of reinforcement, corrosion, and moisture-content, and assess the damage in lining such as voids, fractures, and delamination [27–30]. Generally, tunnels are inspected manually, but some devices have been developed for higher speed data collection and complete cross-section scanning [31–33]. Moreover, other practical problems that typically occur are the loss of contact between the antenna and the surface, the difficulty to maintain a uniform speed, and the presence of conduits and cables through the surface that makes difficult to collect data.

Numerous GPR works can be found in the literature dealing with the assessment of existing structures such as bridges, retaining walls, dikes and dams, and buildings. Regarding the evaluation of stone bridges (road and railways) and stone retaining walls, the method has been successfully employed to detect damage such as cracks/fractures or cavities and moisture content, to estimate thicknesses (ashlars, arches, spandrel walls, etc.), and to investigate filling distribution in masonry and foundations [34–37]. Nevertheless, the interpretation of GPR data is often difficult because of the complexity of stone bridges and the heterogeneity of building materials, which generates diffractions and other unwanted reflections. In concrete bridges, dams, and retaining walls, the GPR findings are mainly focused on estimating cover depth, mapping rebars and other utilities such as joints and dowels, detecting damage on concrete such as cracking or delamination and moisture content, assessing rebar corrosion, and evaluating soil systems and foundations [38–42]. A typical problem when inspecting reinforced concrete structures comes from the presence of steel bars masking the detection of deeper targets. In the case of a tight mesh, collecting data in both polarizations is highly recommended, because the reflections produced by metal targets perpendicular to the scanning direction are weakly seen in data acquired with dipoles parallel to the data-collection direction. Another technical limitation that can be extended to both stone and concrete bridges is the difficult accessibility of the vaults and piers of the structure. With respect to building diagnosis, which includes residential, industrial, and monumental buildings, GPR is an effective tool for thickness estimation in concrete slabs, brick/stone walls, wooden beams, and ashlar [43–45]; detecting hidden structural elements (e.g., floor supporting structures, conduits or post tensioned cables in a concrete slab) [46–48]; mapping radiant (heating) floor [49,50]; damage detection such as cracks, fractures, voids and delamination [51–53]; moisture detection [54,55], mapping pipe supply and water leakage [56,57]; rebar location and corrosion [43,44,58,59]; and estimating the condition of basements/foundations [47].

During the last decade, most of the efforts in GPR developments within this application field include new processing techniques and methodologies for 3D reconstruction and visualization, machine learning techniques for automatic detection (mainly objects with a circular section such as bars and pipes, but also cracks), and data digitization into GIS models [60–67]. Moreover, new multi-antenna systems and array multi-channel antennas have been developed, thus allowing for a dense 3D data collection [68], thus reducing the surveying time and increasing the productivity.

Finally, the recent advances in GPR applied to the monitoring of tree root systems and their impact on the built environment should also be mentioned [69].

Figure 1 shows some examples of GPR application in civil engineering. Figure 1a illustrates an example of pipe detection, highlighting the stronger reflection and inversed polarity by the presence of metal pipes (1) in comparison with the non-metal pipes (2 to 5). Figure 1b presents an example of rigid pavement inspection showing s deteriorated reinforced concrete (RC) slab and the forming cavity below. Figure 1c compares a healthy RC slab consisting of five bars (left) with a deteriorated RC slab showing superficial detachment and rebar at larger travel-time distances (ns) due to higher moisture content (right).

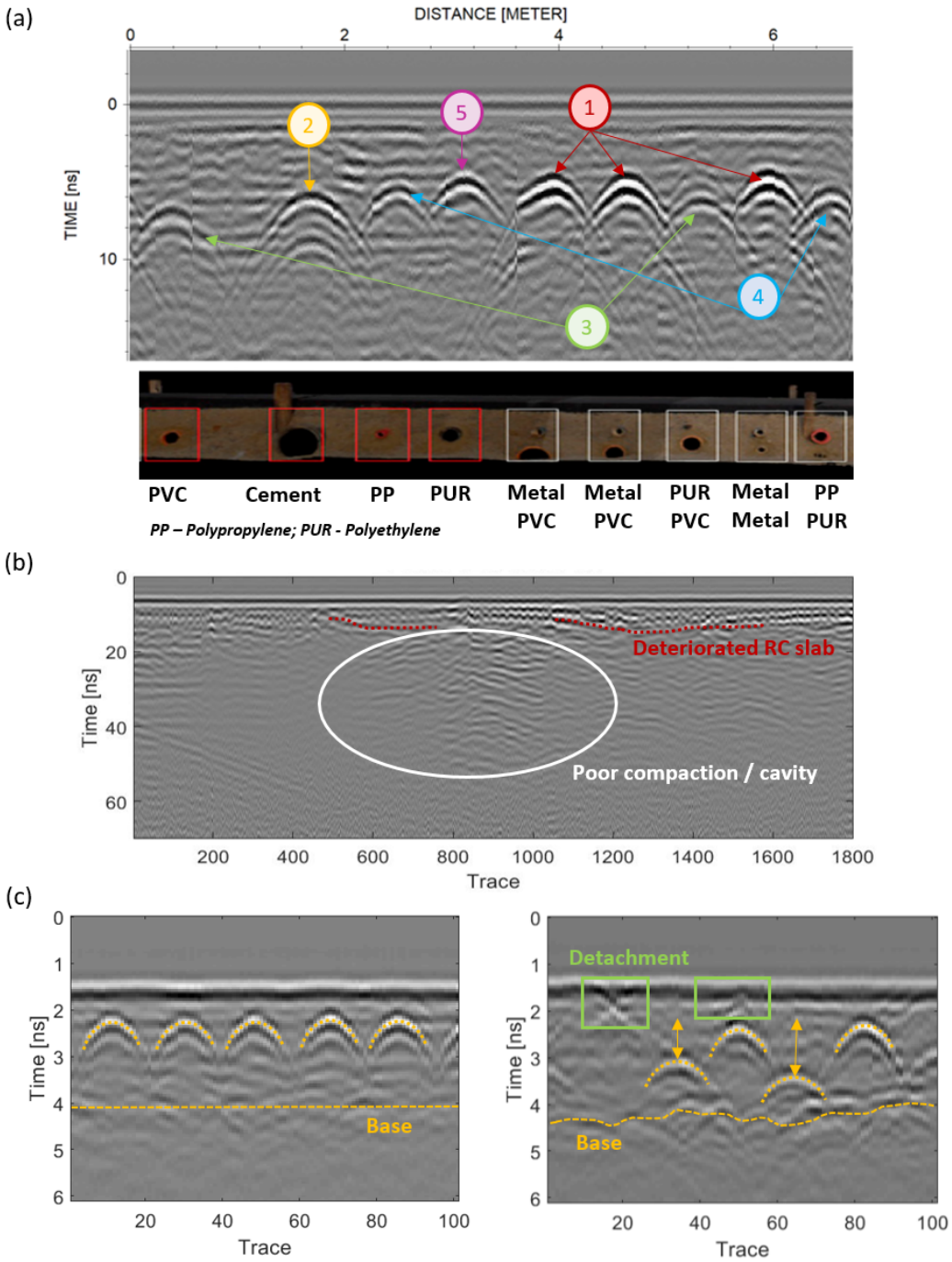

Figure 1. Examples of GPR application in civil engineering: 1 GHz data to detect underground pipes (metal (1), cement (2), PVC (3), polypropylene (4), and polyethylene (5)) (**a**), 500 MHz data in a rigid pavement (**b**), and 2.3 GHz data in building RC slab (**c**). Adapted with permission from Refs. [18,70]. Author's own work and Copyright 2017, Elsevier.

Table 1 provides a list of published reviews on the mentioned GPR civil engineering applications.

Table 1. Published review papers in civil engineering applications.

Application	Title	Year	Ref.
Road pavements/ Infrastructure	GPR monitoring for road transport infrastructure: a systematic review and machine learning insights	2022	[71]
Road/runway pavements; railways; retaining walls; bridges; tunnels	A review of GPR application on transport infrastructures: troubleshooting and best practices	2021	[72]
Moisture content of building materials	Review of moisture measurements in civil engineering with Ground-Penetrating Radar—Applied methods and signal features	2021	[73]
Concrete structures	Non-Destructive Corrosion Inspection of Reinforced Concrete Using Ground-Penetrating Radar: A Review	2021	[74]
Bridges (concrete, masonry, steel)	Condition Monitoring of Bridge Infrastructure Using Non-Contact Testing Technologies: A Comprehensive Review	2020	[75]
Roads, highways, and runways; railways; bridges; tunnels	Ground-Penetrating Radar for the evaluation and monitoring of transport infrastructures	2019	[76]
Buildings; road pavements; bridges; tunnel liners; geotechnical; underground utilities	A review of Ground-Penetrating Radar application in civil engineering: A 30-year journey from Locating and Testing to Imaging and Diagnosis	2018	[77]
Bridge deck	Bridge deck condition assessment by using GPR: a review	2018	[78]
Concrete bridges	Non-destructive test methods for concrete bridges: A review	2016	[79]
Pavement structures	A review of pavement assessment using Ground-Penetrating Radar (GPR)	2008	[80]
Concrete and masonry structures	Review of NDT methods in the assessment of concrete and masonry structures	2001	[81]

The combination of GPR with other non-destructive testing (NDT) techniques has been shown to be beneficial for achieving more robust interpretations and reliable results. According to [72], the other NDTs generally combined with GPR for surveying linear transport infrastructures (roads, runways, railways) are Electrical Resistivity Tomography (ERT), seismic wave propagation and ultrasonic testing (for the detection of cavities, changes in soils properties, and bedrock exploration), load tests such as a Falling Weight Deflectometer (FWD) to evaluate the bearing capacity, and, more recently, the use of Interferometric Synthetic Aperture Radar (InSAR) to subsidence detection. On the other hand, when inspecting masonry and concrete structures, the complementary NDT commonly applied are infrared thermography (IRT) to analyze moisture and shallower cracking, ultrasonic testing or half-cell potential (HCP) to evaluate internal cracking and fractures, as well as concrete corrosion, and ERT or seismic testing to inspect the foundation soils (poor compaction, wet areas), as well as vibrant ambient noise or InSAR to detect structural displacements. Finally, with respect to tunneling inspections, the most typical combination is GPR and seismic to investigate tunnel stability (mainly discontinuities in the rock, loosened materials, and cavities behind lining).

3. GPR Applications in Archeology and Cultural Heritage

Ground-Penetrating Radar represents one of the core methodologies within the landscape of near-surface geophysical techniques addressing archeological prospection and cultural heritage management [82,83]. The GPR method has been successfully employed for a great variety of archeological and cultural heritage applications, such as to locate and map buried archeological artifacts, and to inspect the state of conservation of monumental buildings, statues, frescoes, and mosaics, etc. [84,85].

Within archeology, the development of array multi-channel systems, together with 3D data-processing and visualization, has aided in the acceptance of the technique for archeological prospecting. Multi-channel systems speed up data acquisition and allow full wave-field recording at the same time. Moreover, the use of 3D imaging techniques has produced more realistic and high-resolution images of buried archeological remains, such as villages [86,87], megalithic structures as in the case of Stonehenge [88], and ancient necropolises [89,90], which permits not only finding, but also obtaining volumetric reconstructions, thus allowing archeologists to restore the original appearance of the site [91].

The GPR has also been widely used for preventive damage detection and heritage preservation. The protection and management of monuments must be particularly cautious with the preservation of their singular and historical characters. In this context, GPR has proved to be a powerful non-destructive and non-invasive tool to investigate ancient buildings and monuments. For heritage buildings, GPR was mainly employed to detect damage in façades or walls of churches and cathedrals, such as fractures and cracks, detachments, and moisture [92,93]; to investigate the conservation state of timber beams in floor and ceiling systems [94]; and to locate hidden artifacts such as sarcophagi or tombs [95] and crypts [96]. Furthermore, GPR also allowed for the evaluation of the internal structure and defects in columns [43] and other decorative elements, such as the identification of fractures and iron bolts in the rose window of Troia Cathedral in Southern Italy [97].

Regarding other monumental structures, GPR was successfully applied to monitor fractures and cavities in tombs [98] and statues [99,100]. Ancient masonry arch bridges were also investigated with GPR, which revealed interesting information about hidden arches and former shapes, in addition to other structural details such as thicknesses and the materials' zonification [101–103].

Although there are few examples, GPR has also provided promising results in monitoring the state of conservation of works of art, such as to evaluate the adhesion between different layers and moisture in paintings and frescoes [104] and stratigraphy and water content in mosaics [105,106].

Finally, it was also possible to find some GPR work within the application field of paleontology, particularly for the detection of vertebrate fossils [107,108] and dinosaur sites [109].

Regarding the use of advanced processing such as machine/deep leaning in this field of application, only a few articles are found in the current body of published literature [110,111].

Figure 2 presents some examples of GPR application in archeology and cultural heritage. Figure 2a displays a 3D overlaid GPR image produced at the Roman Site "*Aquis Querquennis*" (Bande, Spain), showing the partial structure of a barrack. Figure 2b presents a sliced 3D cube and the volumetric reconstruction of an ancient underground tunnel consisting of a main corridor and lateral galleries. Figure 2c shows two radargrams acquired with antennas of 2.3 GHz and 1.2 GHz in one anthropomorphic grave of the rock necropolis of San Vítor de Barxacova (Ourense, Spain) showing the interpretation of sub-vertical fractures (red lines).

Table 2 provides a list of published reviews on the mentioned GPR archeological applications.

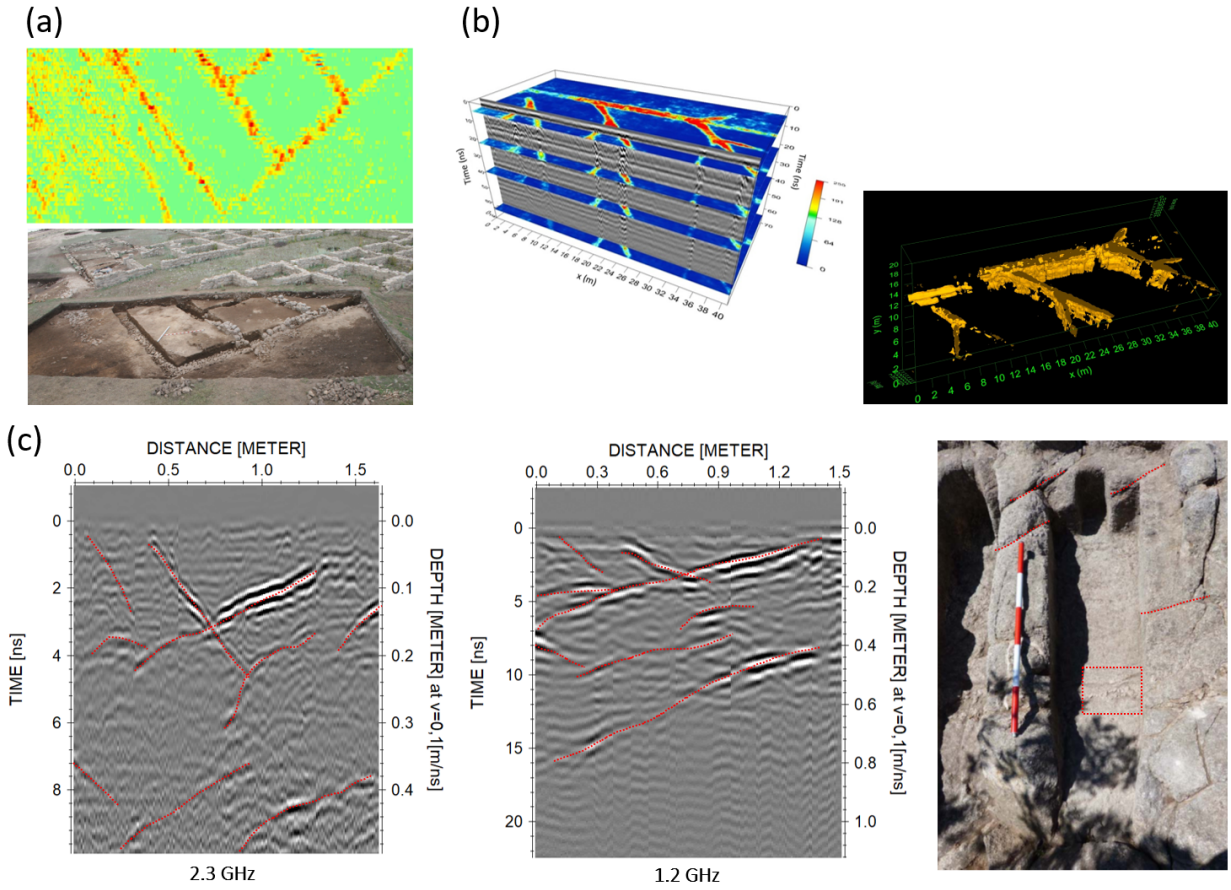

Figure 2. Examples of GPR application in archeology and cultural heritage: 500 MHz overlaid time-slice to detect buried remains at the Roman Site "*Aquis Querquennis*" (**a**), 500 MHz 3D cube and volumetric reconstruction of an ancient underground tunnel (**b**), and 2.3 GHz and 1.2 GHz data to detect internal fractures (red lines) in one anthropomorphic grave of the rock necropolis of San Vítor de Barxacova (**c**). Adapted with permission from [112,113]. Author's own work and Copyright 2014, Elsevier.

Table 2. Published review papers in archeological investigations.

Application	Title	Year	Ref.
Built heritage conditions	Close-range sensing and data fusion for built heritage inspection and monitoring—A review	2021	[114]
Cultural heritage inspection	GPR prospecting of cylindrical structures in cultural heritage applications: a review of geometric issues	2012	[115]
	Non-destructive testing technologies for Cultural Heritage: Overview	2019	[116]
Archeological prospection	Large-area high-resolution Ground-Penetrating Radar measurements for archaeological prospection	2018	[117]
	Sensing archaeology in the north: the use of non-destructive geophysical and remote sensing methods in archaeology in Scandinavian and North Atlantic territories	2020	[118]
	Ground-Penetrating Radar for Archaeology and Cultural-Heritage diagnostics: Activities Carried Out in COST Action TU1208	2018	[119]

Large-scale archeological prospections are typically carried out by combining different geophysical methods, mainly GPR, ERT, and magnetic, but also remote-sensing imagery [85]. The ERT provides complementary results in detecting voids, cavities, tunnels/galleries, and buried structures, while magnetometry allows for the detection of magnetic and conductive bodies in the subsurface (buried remains and fireplaces). In

the case of heritage buildings and other monuments, such as statues, frescoes, etc., the NDTs commonly used together with GPR are: IRT for moisture detection, ultrasonics (pulse-echo/impact-echo) to analyze internal cracking, voids, and delamination, as well as corrosion, and acoustic tomography and seismic reflection to measure elastic parameters and waves velocities in walls and columns [120].

4. GPR Applications in Forensic and Security

Ground-Penetrating Radar (GPR) technology has become an important subsurface prospection tool to assist forensic investigation in a broad range of security applications, from buried explosive threats to human remains detection, as well as locating and tracking people in disaster areas [121,122], mainly due to its high degree of flexibility, which is hardly achievable with other geophysical alternatives [123]; its enhanced operations efficiency, as a consequence of the possibility of rapidly highlighting suspected areas to then be thoroughly searched; and its preservation of the scene, thanks to its non-destructive nature [124].

Applications of GPR are increasingly widening and gaining relevance, not only from a research and development perspective, but also thanks to its regular adoption by a variety of law enforcement agencies, legal and technical surveys operations, and demining platforms, either as a complementary unit or a standalone tool for route and roadside clearance [125–129]. The technology has demonstrated its valuable performance also in search and rescue operations, either in urban or rural scenarios and for the search of human remains or buried evidence. Throughout the years, the technological development of GPR systems has embraced the entire acquisition, processing, and imaging chain, due to the wide variety of challenging scenarios that the methodology has to face and cope with.

In the case of natural catastrophes or man-made disasters, such as earthquakes, avalanches, or buildings collapsing, the priority of search-and-rescue operations is to detect vital signs below the debris piles or the opaque layers as quickly as possible, as the survival time of a trapped person might be very limited. Due to the complex and potentially unstructured subsurface conditions in disaster areas, a visual and manual search is time consuming and error prone, considerations which have pushed the development of easy-to-deploy, real-time, and easy-to-interpret technologies [130,131]. Within this critical domain, two main objectives can be highlighted: the detection of voids that are naturally created during the collapse of a structure and the detection of vital signs and movements [132,133].

From a first-responder perspective, information about the presence of buried voids and cavities is essential to ensure efficient and effective operations; they also represent a critical feature for prioritizing the area that need to be searched. At the same time, subsurface voids, unstable and hidden by nature, are a source of hazard for search-and-rescue operators, given the risk of falling into holes covered by loose rubble and becoming injured. Such subsurface characteristics and associated risks can also be found in the case of avalanche-trapped people, in which case the available time is even more constrained. Despite the highly challenging subsurface conditions, GPR has been researched as a tool to increase situational awareness and reduce search times [134,135]. In both scenarios, research attempts have been made to improve the clarity of GPR profiles and strengthen the magnitude of radar reflections, with the major accomplishments achieved in the characterization of human signatures and automatic localization [136]. The combination of GPR sensors and robotic platforms, such as UAV [137,138] and helicopters, is gaining more and more attention, particularly for scenarios in which the intervention of human operators is limited [130].

Unlike common GPR operations, which essentially focus on the detection of stationary targets, locating human beings is based on target-movement detection. GPR technology has demonstrated its ability to sense slight movements and shallow breathing of a survivor in seconds, making GPR a suitable tool for the detection of trapped people in a disaster area [132,139]. Both continuous-wave radar (CW), exploiting the traditional doppler effect, and ultra-wide band radar (UWB), relying on the time difference of the reflected wave due to the motion of a person, have been successfully employed for survivor detection, the latter exhibiting better performance thanks to a better resolution capability [140–142].

GPR has been proposed as an alternative to classical electromagnetic induction techniques for landmine detection due to a number of advantages, the principal one being the ability to detect landmines with little or no metal content, as long as there is a difference in the electromagnetic contrast between the ground and the target [120,143,144]. In addition, advanced imaging algorithms and data post-processing has allowed not only the localization of the target but also the extraction of valuable features that can pave the way for target recognition and identification [145–149]. However, standalone GPR platforms for antipersonnel landmine detection are less common than their metal detector counterparts, a situation possibly related to the fact that GPR signal interpretation remains a complex task and that the mentioned benefits are often balanced by its susceptibility to clutter [150]. A separate discussion can be developed for military operations, in which GPR is regularly mounted on route clearance convoys [151] for minefield breaching and antitank-mine detection.

The use of GPR for mapping unmarked graves in historical cemeteries, finding clandestine burial sites or hidden bodies, is becoming more common, as can be appreciated by the increasing number of published case studies that have successfully employed the technology [152–154], predominantly to assist search teams. These forensic contexts are highly problematic and challenging for investigators, due to the great uncertainty related to the circumstances surrounding the event and the related expenses in terms of human resource, features which typically result in a low success rate. The adoption of GPR has made it possible to search large areas in minutes, providing accurate information on soil disturbance and modification without altering the site, and allowing the data to be visualized in real time to offer immediate evidence and feedback to the operator [155,156].

The wide variety of possible targets and scenarios in the security application area represents the principal challenge for the development of dedicated GPR-based platforms.

Regarding advances in data processing, algorithms that have been developed are mainly based on automated feature extraction, clutter and unwanted interference removal, and image classification, with the objective of increasing the operator's confidence in the interpretation of the obtained results and to support the labelling activity [157–163].

Figure 3 presents some examples of GPR application in the forensic and demining contexts. Figure 3a displays a radargram produced in a missing person case, in which it is possible to delineate the geological layer (red), the curve roof of the subsurface cave (yellow), and an anomaly due to a possible body (green). Figure 3b presents the results from an experimental test evaluating the performance of GPR methodology in detecting avalanche-trapped people and buried remains. The two results in Figure 3c show the potential of 3D GPR reconstruction for demining applications, not only for accurately delineating the object contour, but also for detecting the presence of internal multiple reflections.

Table 3 provides a list of published reviews on the mentioned GPR-based forensic and security applications.

Table 3. Published review papers in forensic and security applications.

Application	Title	Year	Ref.
Forensic studies	Forensic geophysics: how GPR could help police investigations	2016	[122]
UXO/ERW/IED detection	Ground-Penetrating Radar for Buried Explosive Devices Detection: A Case Studies Review	2021	[164]
AP/AT landmines	Radar Systems for Landmine Detection	2020	[165]
	Ground-Penetrating Radar for Close-in Mine Detection. In Mine Action, The Research Experience of the Royal Military Academy of Belgium	2017	[166]
Avalanche and trapped people.	A review on Ground-Penetrating Radar technology for the detection of buried or trapped victims	2012	[167]
	A Review of Radars to Detect Survivors Buried Under Earthquake Rubble	2017	[168]
Buried remains	The Application of Ground-Penetrating Radar for Forensic Grave Detection	2012	[169]

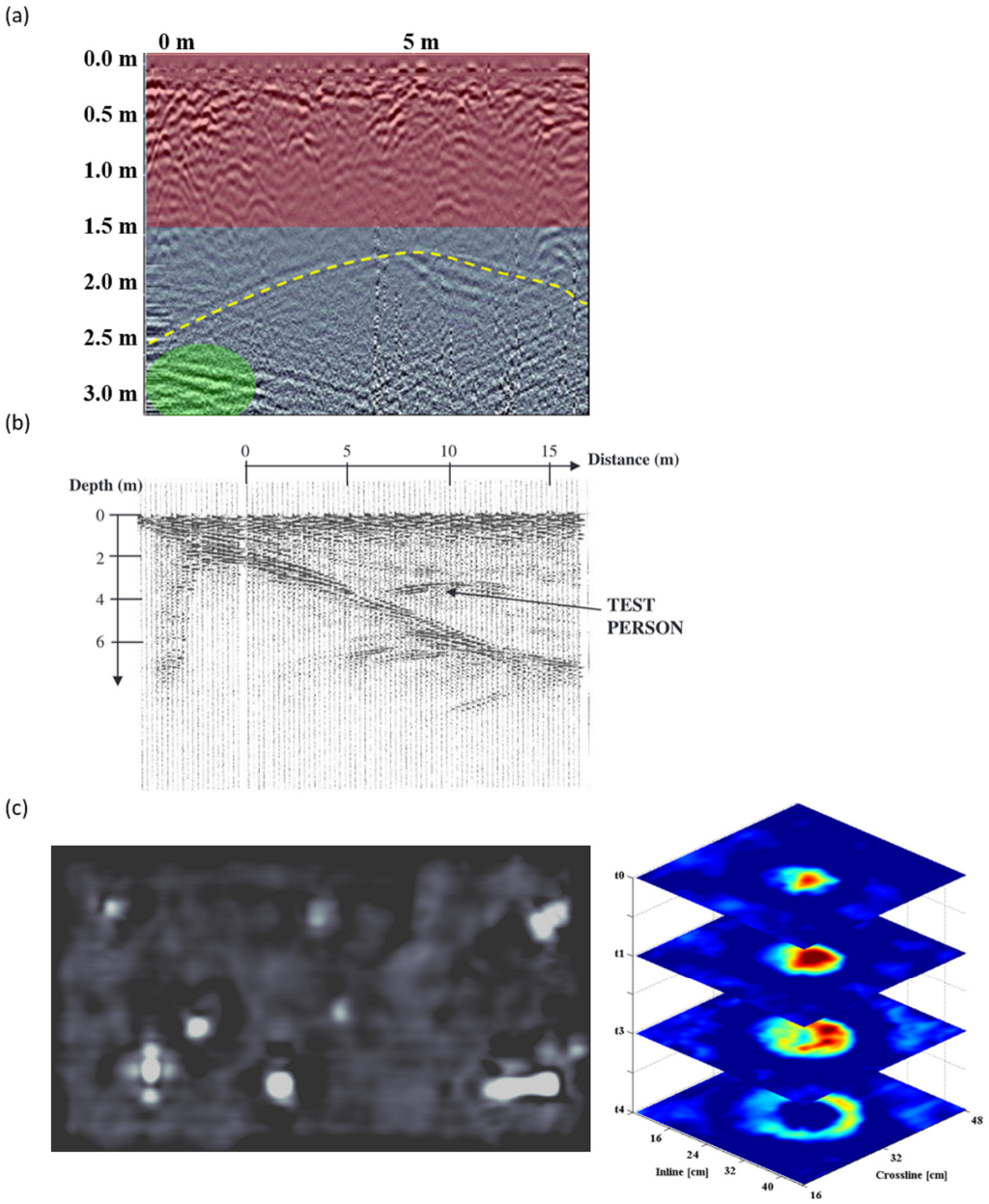

Figure 3. Examples of GPR application in forensic and demining contexts. (**a**) A 500 MHz radargram acquired over the potential location of a missing person (green shadow). (**b**) A 900 MHz radargram showing an example of a cave with a test person. (**c**) Depth slice of a 2 GHz 3D acquisition over a test minefield including inert landmines, mortar shells and rocks. From the same survey, Set of 2 GHz slices of an antipersonnel landmine showing the presence of an internal structure within the landmine volume. Adapted with permission from [122,135]. Copyright 2014, IEEE.

A wide range of geophysical techniques is applied in forensic investigations, the choice being mainly dependent on target size, target type, burial depth, and surrounding soil characteristics. Generally, electrical resistivity and magnetic methods are used to reduce the search area, which could reach several hectares in the case of clandestine burial sites or hidden buried remains, so that most of the resources are concentrated when there is a precise need and evidence, thus saving time from non-contaminated areas (which represent the predominant situation). GPR is then typically deployed for anomaly characterization and identification, thanks to its higher resolution and its capability of reconstructing the exact geometry of the detected object [170,171]. Concerning landmine detection, the majority of sensor integration strategy includes metal detectors and GPR, representing the most

mature solution in terms of technology deployment, but there are examples which also comprise an IR or optical imaging sensor [172]. Finally, for search-and-rescue operations, micro-seismic, and acoustic monitoring has been proposed as an alternative solution [173].

5. GPR Applications in Environmental Investigations

Representing one of its first and core domains of application, GPR methodology has always held promise for enhancing the characterization and monitoring of the subsurface by providing a spatially extensive, non-destructive, non-invasive, and high resolution means of investigation, with respect to alternative solutions [174]. In particular, what has secured the methodology a prominent position is that it can provide high resolution images of the dielectric property variations typically associated with subsurface structures, of the top few tens of meters of the earth with a very dense spatial distribution. Such potential, combined with the capability of delineating the subsurface geometry, has allowed the methodology to play a relevant role in the development of accurate hydrogeologic models of the large-scale stratigraphy of the subsurface. In addition, GPR works almost in real time; it is thus capable of revealing subsurface structures without any time delay during a survey. The technique has been successfully adopted in a variety of environmental and agricultural investigations, not only for extracting qualitative information on the subsurface, but also with the aim of estimating fundamental parameters to obtain a deeper understanding of its heterogeneity and dynamics.

Considering the operating principles of the methodology, GPR is being increasingly used in scenarios where water content, transport, and solutes represent the predominant players, such as hydrogeological site characterization, soil–water content monitoring, hydraulic conductivity estimation, and groundwater studies [175,176].

GPR for hydrogeological studies has mainly embraced the definition of near-surface aquifer geometries and stratigraphic information [177–181], as well as the determination of the water table depth and volumetric water content [182–185]. While the determination of the subsurface geometry is a well-established procedure and can be quantitatively extracted from traditional radargrams, the estimation of soil dielectric properties is performed through the solution of specific petrophysical relationships, which link the measured permittivity properties to the material porosity and moisture content. Hence, substantial research has been carried out to increase the accuracy of such relationships and overcome major limitations in their applications [186,187]. Conceptually related to this field of application is contaminant hydrology, a branch in which GPR has provided a highly efficient means of determining the presence of immiscible contaminants by detecting changes in the subsurface dielectric properties, including salts, hydrocarbons, and other organic materials [188,189]. Research has demonstrated the potential of GPR not only to detect such contaminants in order to plan specific countermeasures, but also for studying the dynamics of contaminant transport processes within natural geologic systems. In addition, when repeated measurements are taken, using a technique commonly called time lapse, GPR surveys enable users to accurately monitor the local impact of remediation measures.

Information on water content, porosity, and soil moisture is also critical within the domain of agriculture and precision farming, where such features have an immediate impact on crop yield, irrigation management, and the environmental effects of farming activities [190–193]. The use of GPR in the agricultural discipline, therefore, has been extensively researched with aims spanning from estimating the limited soil depth restricted by bedrock, hardpan, or water table; determining the root biomass; and mapping local soil attributes affecting agricultural performance, to the characterization of movements of agrochemicals and vadose zones, local soil texture, and layering [194,195].

Ground-Penetrating Radar is an ideal method for glaciological studies, as dry snow and ice are highly transparent to GPR signals, thus providing the most advantageous environment for GPR signal propagation [196]. This has led to an exponential expansion of radar investigations of snow and ice, both ground based as well as adopting airborne survey platforms [197,198]. The main objectives of the application are the determination of

sheet thickness and reconstruction of bed topography, internal layering, and delineation of hydraulic pathways; the detection of crevasses and cavities; and reflectivity computation [199–204]. Significant research has been carried out into the characterization of both temperate and polythermal glaciers, in order to determine local density, ice fabric, and characterizing conductivity variations due to impurities [205,206]. Similar in principle is the application of GPR to the study of permafrost, as geologic materials exhibit very different physical behaviors in the presence of liquid water or ice [207–209]. The importance arises not only from the scientific interest in investigating permafrost distribution and properties, but also from the fact that the knowledge of spatial and temporal variations in freezing and thawing of the ground affect the possibilities of infrastructure expansion and human activities in these regions.

Applications of GPR for surface mining represent a niche and a quite recent expansion of the methodology, in which GPR is gaining acceptance as a rapid geophysical method providing high-resolution information for certain mineral resource evaluation applications [210]. The objective of most GPR surveys for these applications is to provide horizon continuity between existing or planned boreholes, a process that is speculative in nature due to the large variability of layer thicknesses that can exist between even closely spaced boreholes. GPR can be employed to quantify the occurrence of uneconomic boulders and dykes, as well as groundwater tables, for optimizing quarrying activities [211]. For some specific tropical deposits, such as lateritic and bauxitic deposits, high-resolution information on weathering horizons can lead to the definition of resources prior to mining [212]. In addition, the understanding of the subsurface geology of paleo-fluvial environments and correlated placer deposits, and in particular bedrock topography and grain-size distribution, is critical to resource exploration and mine engineering. Finally, iron ore deposits, mineral sands, coal, and kimberlites represent other examples of growing fields of application for GPR surveying [213,214].

In this case, advances in data processing have addressed signal attribute extraction and characterization to associate waveform parameters with specific subsurface features, such as moisture content and volumetric water content, as well as to classify radar results to complement, or even replace, human interpretation [215–218].

Figure 4 presents some examples of GPR applications for environmental studies. Figure 4a displays the 3D geometrical reconstruction of an alluvial aquifer for groundwater flow prediction. Figure 4b presents the interpreted radargram for glacier-bed delineation and ice-thickness estimation. Figure 4c shows a GPR profiles exhibiting deep and highly localized anomalies caused by sediment depression in superficial aquifers due to water percolation. Figure 4d displays a 2D profile including a detected kimberlitic pipe sub-cropping.

Table 4 provides a list of published reviews on the mentioned GPR environmental applications.

Table 4. Published review papers in environmental investigations.

Application	Title	Year	Ref.
Hydrology	Current uses of Ground-Penetrating Radar in groundwater-dependent ecosystems research	2017	[219]
Waste and contaminants	Ground-Penetrating Radar for Environmental Applications	2001	[195]
Soil studies	Application of Ground-Penetrating Radar methods in soil studies: A review	2019	[220]
Agricultural studies	Ground-Penetrating Radar for underground sensing in agriculture: a review	2016	[221]
Ice sounding	Five decades of radioglaciology	2020	[222]
Mining	A review of selected Ground-Penetrating Radar applications to mineral resource evaluations	2012	[223]
Root biomass	Application of Ground-Penetrating Radar for coarse root detection and quantification: a review	2013	[224]

Among the different techniques commonly adopted within the domain, GPR is predominantly combined with ERT, EMI, and hyperspectral sensors, as a consequence of the fact that the majority of applications involve the detection of a water-related physical and chemical parameter or variations in the electrical property of the subsurface. This is particularly true for soil moisture content and contaminant monitoring [225–229]. However, GPR remains probably the most exploited geophysical method for glaciological studies and glacier monitoring, as well as for all other applications in which retrieving the geometrical attributes is a critical and essential task.

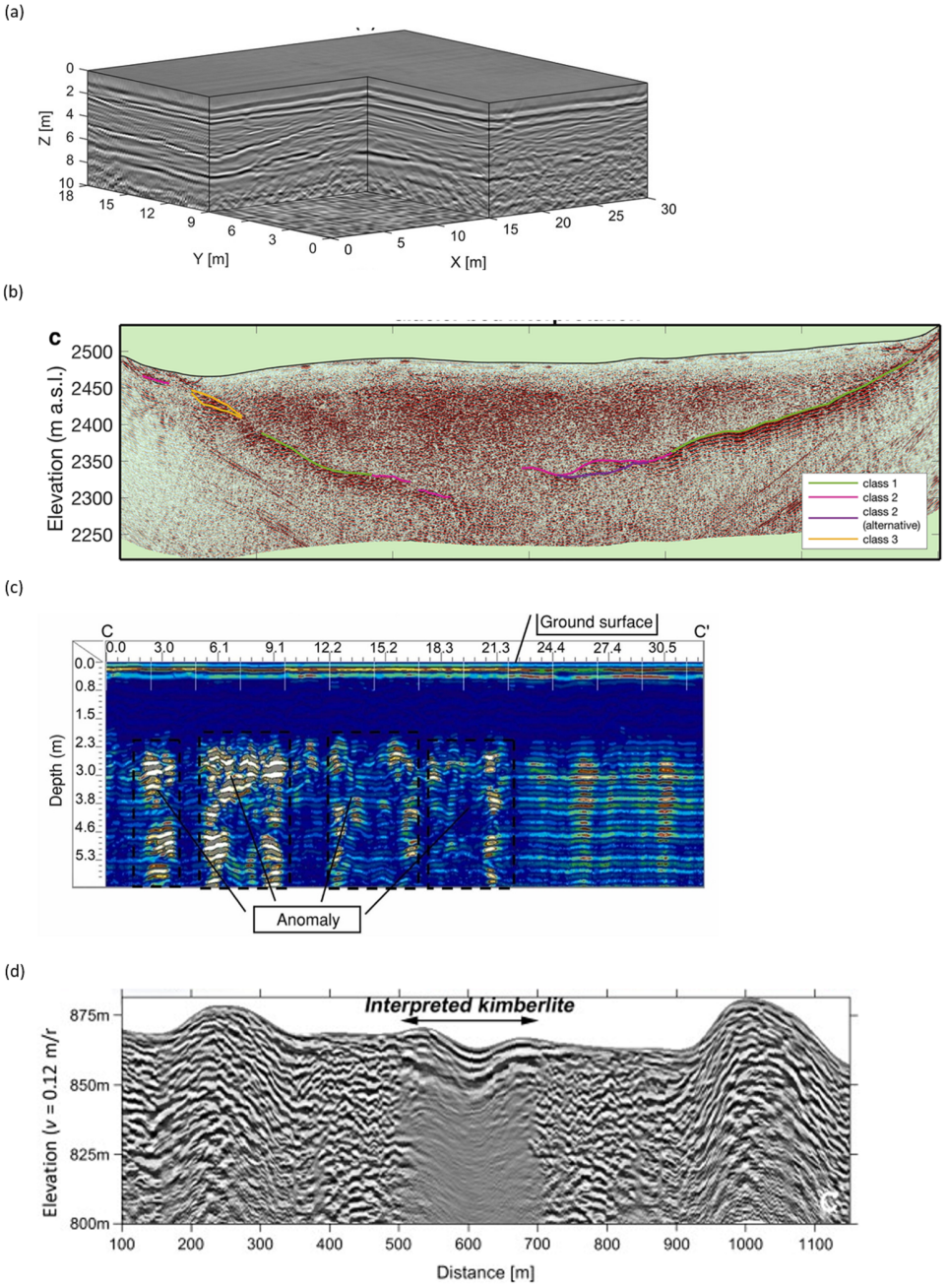

Figure 4. Examples of GPR applications for environmental studies. (**a**) A 100 MHz GPR volume delineating the geometry of an alluvial aquifer and exhibiting the dominant dip of the sediments. (**b**) Glacier bed interpretation and reflection quality classification from a 25 MHz GPR profile over a Swiss valley glacier. (**c**) GPR profiles and location of detected anomalies and sinkhole data from a 270 MHz equipment. (**d**) A 30 MHz radar profile showing the occurrence of a non-diamondiferous kimberlite pipe. Adapted with permission from [178,188,204,223]. Copyright 2012/2022, Elsevier.

6. GPR Applications in Geology

Given the typically strong dielectric and conductivity contrasts between bedrock and overburden, GPR methodology represents an effective tool to detect the interface between the two, thus supporting the definition of the stratigraphic architecture, the sand-body geometry, and correlation and quantification of sedimentary structures [230,231].

GPR has been widely used by sedimentologists to reconstruct past depositional environments and the nature of sedimentary processes in a variety of environmental settings, leading to the development of improved models, especially when combined with cores, trenches, outcrops, and quarry faces. While early comparisons between GPR profiles and outcrop sections were largely qualitative and relied strongly on visual evidence, more recent outcrop analysis has turned its attention to quantitatively determining the causes of GPR reflections [232–236]. Its adoption is also related to the rapidity of data collection and the apparent analogy with its seismic reflection counterpart.

Several GPR applications to palaeo-seismological studies for imaging active faults are found in the literature, with varying degrees of success depending on the local lithologies and network geometry [237,238]. Not only can it be stated that GPR could represent a valuable pre-trenching tool for paleo-seismic surveys, but also that the technique has shown great potential in tracing fault segments along strikes, assessing variations in their displacements, and, hence, determining their chronology. Within this domain, geometric and morphological attributes have been widely developed to highlight the features of fault zones that are hardly visible in standard GPR profiles [239,240].

The detection of fractures of various scale, from millimetric up to a decametric scale, represents another topic widely researched with GPR, where its geometrical reconstruction capability has made it a valuable tool for characterizing mining sites and rock masses, improving quarries and extraction processes, and determining unstable rock slopes [241–244]. Another successful application of GPR within this domain is the determination of fracture openings and fillings [245–247], crucial for several environmental and engineering applications, including the accessibility of geothermal energy. Fractures and faults represent the primary conduits for the transport of heated fluids needed for geothermal energy, and therefore a detailed knowledge on the fracture network is essential to increase the efficiency of the energy-transition process [248–252].

The favorable setting of dune sands for GPR investigations, and in particular the extended and spatially continuous sedimentary structures within it and the low conductivity typically exhibited by aeolian sands, have been known for decades [253,254]. Dune are essentially hills of sand built up and shaped by the wind via a number of processes including erosion, transportation, and deposition, and understanding of them is critical in several fields, including sedimentology, palaeoclimatology, aquifer characterization, and groundwater studies. Within this context, GPR has allowed for quick and non-invasive operations, as well as high-resolution 3D results [255]. Many studies have shown the importance of GPR as a tool for studying and characterizing the internal structures of sand-bodies' elements. In particular, the successful adoption of the technique has mainly targeted the geometrical reconstruction of the internal sedimentary structures of aeolian dunes, to define the relative chronology of sand deposition, dune development, and migration, as well as studies on the impact that grain size-distribution, grain shapes, and compaction processes might have on the radar results [256–258].

In addition, sediment analysis represents a relevant task of lacustrine investigations, where freshwater allows for improved wave penetration and image resolution [259–261]. With respect to conventional underwater mapping methods, GPR represents a faster and more reliable solution, particularly in a shallow water context, capable of providing a continuous cross-section of the lake bottom and the underlying sediment column [262–266]. Waterborne GPR mapping of lakes has several objectives, including studies of sedimentation environments and stratigraphic boundaries [267,268], the estimation of a sedimentation rate and volume of lacustrine sediments [269], and the tracing of tectonic faults and displacements beneath the lake [270], improving the understanding of the evolution of water

bodies at a local scale. GPR has also been applied to delineate reference horizons and local geophysical features [271].

Finally, over the last decade, the possible use of GPR methodology for planetary exploration has regained favor as a consequence of the continuous technological advances and the recent rover missions that have highlighted the importance of GPR equipment in mapping the subsurface characteristics of landing sites, including the geometry of sedimentary deposits and subsurface stratigraphy, as well as to retrieve scientifically relevant information on planetary soils [272–277]. Though orbiting radars have been routinely adopted since the end of the twentieth century, the Chinese Chang'E-3 (CE-3) mission in 2013 represented the first attempt to physically deploy a GPR platform over the moon's surface [278,279], and the equipped 500 MHz antenna system was capable of providing detailed information on the moon's subsurface down to a depth of 10 m [280,281], boosting the widespread adoption of GPR for planetary exploration. More recently, the Chang'E-4 mission in 2019 was the first successful landing on the far side of the moon [282], providing, therefore, an unprecedented opportunity to gather knowledge on the subsurface structure of the lunar far side. As a reference, results have highlighted significant geological differences between the two landing sites, underlining once again the potential that GPR technology could bring to the planetary exploration field [283–286]. More recently, the NASA Mars 2020 Perseverance Rover mission [287,288] has, for the first time, deployed a GPR platform on the surface of Mars [289,290] to assess the depth and extent of the regolith and to characterize the stratigraphic section by identifying material dielectric properties. On top of that, within this emerging field, GPR could provide critical information on the geological processes that formed the sedimentary surface of the planet and its past exposure history, as well as signs of past life.

Across these field of applications, automated machine learning and classification models have been applied to process GPR data with the aim of classifying geological structures, estimating dielectric variations, and identifying geological boundaries [291–295].

Figure 5 presents some examples of GPR applications in geological horizon reconstruction. Figure 5a displays a radar section acquired over a coastal dune to reconstruct the stratigraphical beddings and erosional surfaces composing its internal structures, along with its interpretation and stratigraphic model. Figure 5b presents a horizontal depth slice showing the presence of deep diffraction events likely related to sub-vertical fractures, fracture wall intersections, or geological heterogeneities. Figure 5c shows the results from a water-penetrating radar experiment aimed at locating a 17th Century sunken trackway. Figure 5d displays the model of the moon subsurface geological structure at the CE-4 landing site as inferred from GPR measurements.

Table 5 provides a list of published reviews on the mentioned GPR geological applications.

Table 5. Published review papers in geological investigations.

Application	Title	Year	Ref.
Fractures/faults	The use of Ground-Penetrating Radar to distinguish between seismic and non-seismic hazards in hard rock mining	2020	[296]
Stratigraphic studies	Ground-Penetrating Radar and its use in sedimentology: principles, problems and progress.	2004	[297]
	A review of Ground-Penetrating Radar studies related to peatland stratigraphy with a case study on the determination of peat thickness in a northern boreal fen in Quebec, Canada	2013	[298]
Bathymetry	Water penetrating radar	2021	[299]
Sand bodies	Radar suitability in aeolian sand dunes—A global review	2012	[300]
Planetary exploration	Applications of Radar Systems in Planetary Sciences: An Overview	2015	[301]

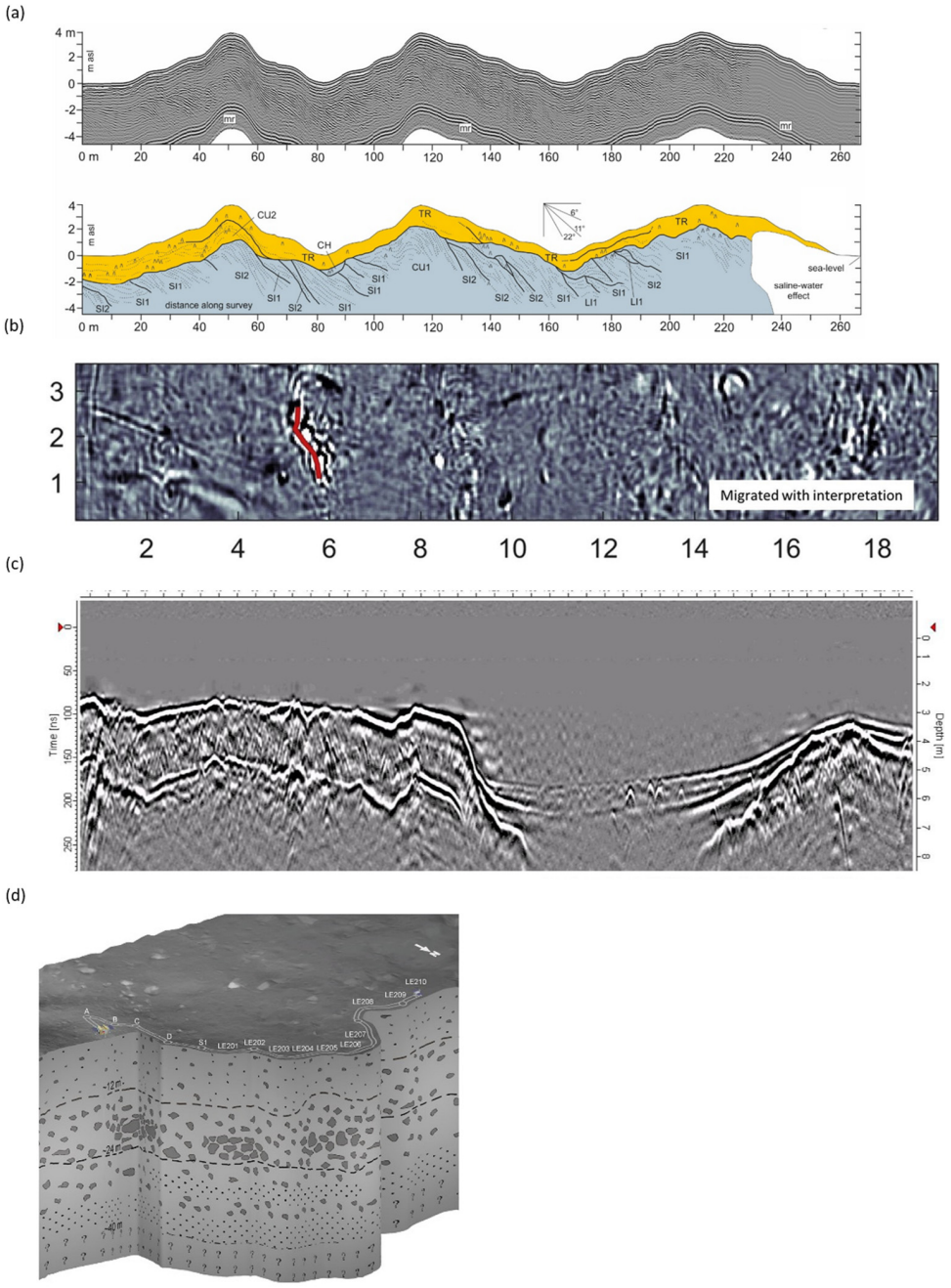

Figure 5. Examples of GPR application in geology. (**a**) A 600 MHz radargram acquired over a coastal dune characterized by erosion, accretion, and equilibrium to delineate its internal stratigraphy. Corresponding model highlighting the upper Aeolian unit (yellow) and lower marine unit (blue). (**b**) A 450 MHz GPR depth slice (1.32 m depth) over a vertical and sub-vertical fracture network showing the typical diffraction events generated by such horizons. (**c**) The 100 MHz unshielded antennas for lake-bottom profiling investigations. (**d**) Subsurface internal structure at the landing site as inferable from the Chang'E-4 500 MHz GPR survey over the far side of the moon. Adapted with permission from [245,253,286,299]. Copyright 2020/2021, Elsevier.

Considering that the geophysical response of complex geological bodies exhibits different physical properties due to the fact that such horizons are composed of a combination of layers with contrasting properties and are caused by a host of geological, geotechnical, and climatic factors, a multidisciplinary approach is often recommended to gather an in-depth understanding of the features. Typically, this involves the GPR technique as the primary method to determine the velocity and geometrical attributes of the subsur-

face, while electrical resistivity tomography and seismic reflection and refraction often work as complementary methods [302–309], due to their limited resolutions and mediocre stratum-detection performance, in particular for the shallow subsurface.

7. Conclusions and Further Perspectives

This comprehensive, though not exhaustive, survey of the application areas in which GPR has proven to be a technological and operational breakthrough essentially shows that the applications of GPR are almost endless. Whether the objective of the survey is to reconstruct complex subsurface geometries or to determine variations in the soil permittivity properties, the methodology represents a key player within the landscapes of near-surface geophysical techniques.

However, it also reveals the main challenge common to all: the need of a deciphering key capable of translating GPR information into useful quantitative information on the reflectivity coefficients for the end users, that is to say, mapping the apparent values exhibited by the radar data to the actual permittivity values, so that it will be possible to unravel complex human–environment interactions. In addition, this is where much remains to be completed to effectively bridge the gap between interpretation and identification. Such an ability could be even more improved by developing advanced learning processing techniques and algorithms derived from computer vision research, features which are still confined to a relatively limited applicability. In particular, the automated extraction of information from GPR image is a long-awaited capability that is expected to reduce the dependency of GPR results on the operator's familiarity and skills, but its performance is still hindered by the presence of subsurface heterogeneities or weak target scattering, two attributes not so uncommon within the GPR domain.

On top of that, it has been also shown that there is a continuous need for enhancing the operativity of GPR by deploying advanced surveying platforms (including unmanned aerial and robotics, to address the most unfavorable scenarios or make it possible to survey hazardous areas) and by developing suitable multi-sensor platforms and related multi-sensor data fusion to increase the available information on the surveyed site. This last consideration is a fundamental consequence of the multifaceted nature of typical geophysical problems. An example of this can be found within the humanitarian demining domain, in which operation performance has greatly benefited from the combination of GPR and metal detector technologies, even if the two sensors are typically treated as independent. Finally, due to the severe limitations in signal penetration and consequently in the achievable resolution, unmanned aerial platforms have frequently failed not only in detecting the target of interest, even when shallowly buried, but also in generating reliable underground images due to several uncertainties in the image-formation process. Still, a number of successful applications of airborne GPR can be found, particularly when the aim is to delineate large subsurface features in a homogeneous context.

In conclusion, although GPR technology is established, it is capable of further developments to enable the continued classification of evolving targets and the continued reduction of the size, weight, and power of equipment, at the same time reducing the need for human presence and supervision.

Author Contributions: Conceptualization, F.L., F.P. and M.S.; writing—original draft preparation, F.L., F.P. and M.S.; writing—review and editing, F.L., F.P. and M.S. All authors have read and agreed to the published version of the manuscript.

Funding: M. Solla acknowledges the grant RYC2019–026604–I funded by MCIN/AEI/10.13039/50110 0011033 and by "ESF Investing in your future". This work has received funding from the Xunta de Galicia—GAIN—through the project ENDITí (Ref. ED431F 2021/08).

Data Availability Statement: Not applicable.

Conflicts of Interest: The authors declare no conflict of interest. The funders had no role in the design of the study; in the collection, analyses, or interpretation of data; in the writing of the manuscript, or in the decision to publish the results.

References

1. Stern, W. Versuch einer elektrodynamischen dickenmessung von gletschereis. *Gerlands Beitr. Geophys.* **1929**, *27*, 292–333.
2. Waite, A.; Schmidt, S. Gross Errors in Height Indication from Pulsed Radar Altimeters Operating over Thick Ice or Snow. *Proc. IRE* **1962**, *50*, 1515–1520. [CrossRef]
3. Porcello, L.; Jordan, R.; Zelenka, J.; Adams, G.; Phillips, R.; Brown, W.; Ward, S.; Jackson, P. The Apollo lunar sounder radar system. *Proc. IEEE* **1974**, *62*, 769–783. [CrossRef]
4. Sloan, S. A current look at geophysical detection of illicit tunnels. *Geophysics* **2015**, *34*, 154–158. [CrossRef]
5. Ballard, R.F. Tunnel Detection. Geotechnical Laboratory U. S. Army Engineer Waterways Experiment Station. 1982. Available online: www.apps.dtic.mil/sti/citations/ADA121447 (accessed on 3 May 2022).
6. Nilsson, B. Two Topics in Electromagnetic Radiation Field Prospecting. Ph.D. Thesis, University of Lulea, Lulea, Sweden, 1978.
7. BBC News. Available online: http://news.bbc.co.uk/2/hi/uk_news/1019682.stm (accessed on 3 May 2022).
8. BBC News. Available online: http://news.bbc.co.uk/1/hi/uk/7103836.stm (accessed on 3 May 2022).
9. Travassos, X.L.; Avila, S.L.; Adriano, R.L.D.S.; Ida, N. A Review of Ground-Penetrating Radar Antenna Design and Optimization. *J. Microw. Optoelectron. Electromagn. Appl.* **2018**, *17*, 385–402. [CrossRef]
10. Diamanti, N.; Redman, J.D.; Hogan, C.M.; Annan, A.P. Air-launched GPR depth of investigation. In Proceedings of the 18th International Conference on Ground-Penetrating Radar, Golden, CO, USA, 14–19 June 2020; pp. 228–231. [CrossRef]
11. Diamanti, N.; Annan, A.P. Air-launched and ground-coupled GPR data. In Proceedings of the 2017 11th European Conference on Antennas and Propagation (EUCAP), Paris, France, 19–24 March 2017; pp. 1694–1698. [CrossRef]
12. Van De Vijver, E.; De Pue, J.; Cornelis, W.; Van Meirvenne, M. Comparison of air-launched and ground-coupled configurations of SFCW GPR in time, frequency and wavelet domain. In Proceedings of the EGU General Assembly Conference Abstracts, Vienna, Austria, 12–17 April 2015; p. 10038.
13. Benedetto, L.A.; Pajewski, L. Civil Engineering Applications of Ground-Penetrating Radar. In *Transactions in Civil and Environmental Engineering*; Springer International: New York, NY, USA, 2015.
14. Dinh, K.; Gucunski, N.; Zayed, T. Automated visualization of concrete bridge deck condition from GPR data. *NDT E Int.* **2018**, *102*, 120–128. [CrossRef]
15. Šarlah, N.; Podobnikar, T.; Ambrožič, T.; Mušič, B. Application of Kinematic GPR-TPS Model with High 3D Georeference Accuracy for Underground Utility Infrastructure Mapping: A Case Study from Urban Sites in Celje, Slovenia. *Remote Sens.* **2020**, *12*, 1228. [CrossRef]
16. Ayala-Cabrera, D.; Herrera, M.; Izquierdo, J.; Pérez-García, R. Location of buried plastic pipes using multi-agent support based on GPR images. *J. Appl. Geophys.* **2011**, *75*, 679–686. [CrossRef]
17. Rasol, M.; Pérez-Gracia, V.; Solla, M.; Pais, J.C.; Fernandes, F.M.; Santos, C. An experimental and numerical approach to combine Ground-Penetrating Radar and computational modeling for the identification of early cracking in cement concrete pavements. *NDT E Int.* **2020**, *115*, 102293. [CrossRef]
18. Solla, M.; Fernández, N. GPR analysis to detect subsidence: A case study on a loaded reinforced concrete pavement. *Int. J. Pavement Eng.* **2022**, 1–15. [CrossRef]
19. Rasol, M.A.; Pérez-Gracia, V.; Fernandes, F.M.; Pais, J.C.; Solla, M.; Santos, C. NDT assessment of rigid pavement damages with Ground-Penetrating Radar: Laboratory and field tests. *Int. J. Pavement Eng.* **2020**, *23*, 900–915. [CrossRef]
20. Fernandes, F.; Fernandes, A.; Pais, J. Assessment of the density and moisture content of asphalt mixtures of road pavements. *Constr. Build. Mater.* **2017**, *154*, 1216–1225. [CrossRef]
21. Baltrušaitis, A.; Vaitkus, A.; Smirnovs, J. Asphalt Layer Density and Air Voids Content: GPR and Laboratory Testing Data Reliance. *Balt. J. Road Bridg. Eng.* **2020**, *15*, 93–110. [CrossRef]
22. Alani, A.M.; Aboutalebi, M.; Kilic, G. Applications of Ground-Penetrating Radar (GPR) in bridge deck monitoring and assessment. *J. Appl. Geophys.* **2013**, *97*, 45–54. [CrossRef]
23. Liu, H.; Deng, Z.; Han, F.; Xia, Y.; Liu, Q.H.; Sato, M. Time-frequency analysis of air-coupled GPR data for identification of delamination between pavement layers. *Constr. Build. Mater.* **2017**, *154*, 1207–1215. [CrossRef]
24. Al-Qadi, I.L.; Xie, W.; Jones, D.L.; Roberts, R. Development of a time–frequency approach to quantify railroad ballast fouling condition using ultra-wide band Ground-Penetrating Radar data. *Int. J. Pavement Eng.* **2010**, *11*, 269–279. [CrossRef]
25. Plati, C.; Loizos, A.; Papavasiliou, V. Inspection of railroad ballast using geophysical method. *Int. J. Pavement Eng.* **2010**, *11*, 309–317. [CrossRef]
26. De Bold, R.; O'Connor, G.; Morrissey, J.; Forde, M. Benchmarking large scale GPR experiments on railway ballast. *Constr. Build. Mater.* **2015**, *92*, 31–42. [CrossRef]
27. Abraham, O.; Dérobert, X. Non-destructive testing of fired tunnel walls: The Mont-Blanc Tunnel case study. *NDT E Int.* **2003**, *36*, 411–418. [CrossRef]
28. Parkinson, G.; Ékes, C. Ground-Penetrating Radar Evaluation of Concrete Tunnel Linings. In Proceedings of the 12th International Conference Ground-Penetrating Radar (GPR), Birmingham, UK, 16–19 June 2008.
29. Zhang, F.; Xie, X.; Huang, H.-W. Application of Ground-Penetrating Radar in grouting evaluation for shield tunnel construction. *Tunn. Undergr. Space Technol.* **2010**, *25*, 99–107. [CrossRef]
30. Prego, F.J.; Solla, M.; Núñez-Nieto, X.; Arias, P. Assessing the Applicability of Ground-Penetrating Radar to Quality Control in Tunneling Construction. *J. Constr. Eng. Manag.* **2016**, *142*, 06015006. [CrossRef]

31. Balaguer, C.; Montero, R.; Victores, J.G.; Martínez, S.; Jardón, A. Towards fully automated tunnel inspection: A survey and future trends. In Proceedings of the 31st International Symposium on Automation and Robotics in Construction and Mining (ISARC 2014), Sydney, Australia, 9–11 July 2014. [CrossRef]
32. Xie, X.Y.; Chen, Y.F.; Zhou, B. Data processing of backfill grouting detected by GPR in shield tunnel and research on equipment of GPR antenna. In Proceedings of the 16th International Conference on Ground-Penetrating Radar (GPR), Hong Kong, China, 13–16 June 2016. [CrossRef]
33. Zan, Y.W.; Su, G.F.; Li, Z.L. A Train-mounted GPR System for Fast and Efficient Monitoring of Tunnel Health Conditions. In Proceedings of the 16th International Conference on Ground-Penetrating Radar (GPR), Hong Kong, China, 13–16 June 2016. [CrossRef]
34. Trela, C.; Wöstmann, J.; Kruschwitz, S. Contribution of radar measurements to the inspection and condition assessment of railway bridges—Case study at a historic masonry arch bridge in Oleśnica/Poland. *WIT Trans. Built Environ.* **2008**, *97*, 535–544. [CrossRef]
35. Ukleja, J.; Bęben, D.; Anigacz, W. Determination of the railway retaining wall dimensions and its foundation in difficult terrain and utility. *AGH J. Min. Geoengin.* **2012**, *36*, 299–308.
36. Solla, M.; Lorenzo, H.; Rial, F.I.; Novo, A. Ground-Penetrating Radar for the structural evaluation of masonry bridges: Results and interpretational tools. *Constr. Build. Mater.* **2012**, *29*, 458–465. [CrossRef]
37. Conde, B.; Ramos, L.F.; Oliveira, D.V.; Riveiro, B.; Solla, M. Structural assessment of masonry arch bridges by combination of non-destructive testing techniques and three-dimensional numerical modelling: Application to Vilanova bridge. *Eng. Struct.* **2017**, *148*, 621–638. [CrossRef]
38. Hugenschmidt, J.; Mastrangelo, R. GPR inspection of concrete bridges. *Cem. Concr. Compos.* **2006**, *28*, 384–392. [CrossRef]
39. Hugenschmidt, J.; Kalogeropoulos, A. The inspection of retaining walls using GPR. *J. Appl. Geophys.* **2009**, *67*, 335–344. [CrossRef]
40. Loperte, A.; Bavusi, M.; Cerverizzo, G.; Lapenna, V.; Soldovieri, F. Ground-Penetrating Radar in Dam Monitoring: The Test Case of Acerenza (Southern Italy). *Int. J. Geophys.* **2011**, *2011*, 654194. [CrossRef]
41. Diamanti, N.; Annan, A.P.; Redman, J.D. Concrete Bridge Deck Deterioration Assessment Using Ground-Penetrating Radar (GPR). *J. Environ. Eng. Geophys.* **2017**, *22*, 121–132. [CrossRef]
42. Rathod, H.; Debeck, S.; Gupta, R.; Chow, B. Applicability of GPR and a rebar detector to obtain rebar information of existing concrete structures. *Case Stud. Constr. Mater.* **2019**, *11*, e00240. [CrossRef]
43. Pérez-Gracia, V.; García, F.G.; Abad, I.R. GPR evaluation of the damage found in the reinforced concrete base of a block of flats: A case study. *NDT E Int.* **2008**, *41*, 341–353. [CrossRef]
44. Pérez-Gracia, V.; Caselles, O.; Clapes, J.; Santos-Assuncao, S. GPR building inspection: Examples of building structures assessed with Ground-Penetrating Radar. In Proceedings of the 9th International Workshop on Advanced Ground-Penetrating Radar (IWAGPR), Edinburg, UK, 28–30 June 2017; pp. 1–4. [CrossRef]
45. Solla, M.; Gonçalves, L.; Gonçalves, G.; Francisco, C.; Puente, I.; Providência, P.; Gaspar, F.; Rodrigues, H. A Building Information Modeling Approach to Integrate Geomatic Data for the Documentation and Preservation of Cultural Heritage. *Remote Sens.* **2020**, *12*, 4028. [CrossRef]
46. Gehrig, M.D.; Morris, D.V.; Bryant, J.T. Ground-Penetrating Radar for Concrete Evaluation Studies. In Proceedings of the Foundation Performance Association Meeting, London, UK, 24 March 2004.
47. Capozzoli, L.; De Martino, G.; Polemio, M.; Rizzo, E. Geophysical Techniques for Monitoring Settlement Phenomena Occurring in Reinforced Concrete Buildings. *Surv. Geophys.* **2019**, *41*, 575–604. [CrossRef]
48. Pérez-Gracia, V.; Gónzalez-Drigo, R.; Di Capua, D.; Pujades, L.G. Experimental analysis of the resolution in shallow GPR survey. In Proceedings of the SPIE Remote Sensing for Environmental Monitoring, GIS Applications, and Geology VII, Florence, Italy, 17–20 September 2007; SPIE: Bellingham, WA, USA, 2007; Volume 6749, p. 67492M. [CrossRef]
49. Lopez, S.L.; Carracelas, M.S.; Vilariño, L.D.; González, J.A. Inspection of radiant heating floor applying non-destructive testing techniques: GPR and IRT. *DYNA* **2015**, *82*, 221–226. [CrossRef]
50. Rucka, M.; Wojtczak, E.; Zielińska, M. Interpolation methods in GPR tomographic imaging of linear and volume anomalies for cultural heritage diagnostics. *Measurement* **2020**, *154*, 107494. [CrossRef]
51. Cotič, P.; Jagličić, Z.; Bosiljkov, V.; Niederleithinger, E. GPR and IRT thermography for near-surface defect detection in building structures. In Proceedings of the XII Int Conference of the Slovenian Society for Non-Destructive Testing, Portorož, Slovenia, 4–6 September 2013.
52. Çağlar Yalçıner, C.; Büyüksaraç, A.; Kurban, Y.C. Non-destructive damage analysis in Kariye (Chora) Museum as a cultural heritage building. *J. Appl. Geophys.* **2019**, *171*, 103874. [CrossRef]
53. Negri, S.; Aiello, M. High-resolution GPR survey for masonry wall diagnostics. *J. Build. Eng.* **2020**, *33*, 101817. [CrossRef]
54. Agliata, R.; Bogaard, T.A.; Greco, R.; Mollo, L.; Slob, E.; Steele-Dunne, S.C. Non-invasive estimation of moisture content in tuff bricks by GPR. *Constr. Build. Mater.* **2018**, *160*, 698–706. [CrossRef]
55. Garrido, I.; Solla, M.; Lagüela, S.; Fernández, N. IRT and GPR Techniques for Moisture Detection and Characterisation in Buildings. *Sensors* **2020**, *20*, 6421. [CrossRef]
56. Lai, W.W.; Ho, M.L.-Y.; Chang, R.K.; Sham, J.F.C.; Poon, C.S. Tracing and imaging minor water seepage of concealed PVC pipe in a reinforced concrete wall by high-frequency Ground-Penetrating Radar. *Constr. Build. Mater.* **2017**, *151*, 840–847. [CrossRef]
57. Lualdi, M.; Lombardi, F. Utilities detection through the sum of orthogonal polarization in 3D georadar surveys. *Near Surf. Geophys.* **2010**, *13*, 73–82. [CrossRef]

58. Taştan, E.; Koşaroğlu, K.; Bilim, F. Identifying of structural elements of buildings using Ground-Penetrating Radar (GPR): A case study of the Cumhuriyet University, Turkey. *J. Sci. Technol.* **2017**, *7*, 22–26. [CrossRef]
59. Solla, M.; Lagüela, S.; Fernández, N.; Garrido, I. Assessing Rebar Corrosion through the Combination of Nondestructive GPR and IRT Methodologies. *Remote Sens.* **2019**, *11*, 1705. [CrossRef]
60. Asadi, P.; Gindy, M.; Alvarez, M. A Machine Learning Based Approach for Automatic Rebar Detection and Quantification of Deterioration in Concrete Bridge Deck Ground-Penetrating Radar B-scan Images. *KSCE J. Civ. Eng.* **2019**, *23*, 2618–2627. [CrossRef]
61. Kim, N.; Kim, S.; An, Y.-K.; Lee, J.-J. A novel 3D GPR image arrangement for deep learning-based underground object classification. *Int. J. Pavement Eng.* **2019**, *22*, 740–751. [CrossRef]
62. Liu, H.; Lin, C.; Cui, J.; Fan, L.; Xie, X.; Spencer, B.F. Detection and localization of rebar in concrete by deep learning using Ground-Penetrating Radar. *Autom. Constr.* **2020**, *118*, 103279. [CrossRef]
63. Tong, Z.; Gao, J.; Yuan, D. Advances of deep learning applications in Ground-Penetrating Radar: A survey. *Constr. Build. Mater.* **2020**, *258*, 120371. [CrossRef]
64. Mertens, L.; Persico, R.; Matera, L.; Lambot, S. Automated Detection of Reflection Hyperbolas in Complex GPR Images With No A Priori Knowledge on the Medium. *IEEE Trans. Geosci. Remote Sens.* **2015**, *54*, 580–596. [CrossRef]
65. Kim, N.; Kim, S.; An, Y.-K.; Lee, J.-J. Triplanar Imaging of 3-D GPR Data for Deep-Learning-Based Underground Object Detection. *IEEE J. Sel. Top. Appl. Earth Obs. Remote Sens.* **2019**, *12*, 4446–4456. [CrossRef]
66. Feng, J.; Yang, L.; Hoxha, E.; Sanakov, D.; Sotnikov, S.; Xiao, J. GPR-based Model Reconstruction System for Underground Utilities Using GPRNet. In Proceedings of the 2021 IEEE International Conference on Robotics and Automation (ICRA), Xi'an, China, 30 May–5 June 2021; pp. 845–851. [CrossRef]
67. Yamaguchi, T.; Mizutani, T.; Nagayama, T. Mapping Subsurface Utility Pipes by 3-D Convolutional Neural Network and Kirchhoff Migration Using GPR Images. *IEEE Trans. Geosci. Remote Sens.* **2020**, *59*, 6525–6536. [CrossRef]
68. Gabryś, M.; Ortyl, Ł. Georeferencing of Multi-Channel GPR—Accuracy and Efficiency of Mapping of Underground Utility Networks. *Remote Sens.* **2020**, *12*, 2945. [CrossRef]
69. Nichols, P.; McCallum, A.; Lucke, T. Using Ground-Penetrating Radar to locate and categorise tree roots under urban pavements. *Urban For. Urban Green.* **2017**, *27*, 9–14. [CrossRef]
70. Prego, F.; Solla, M.; Puente, I.; Arias, P. Efficient GPR data acquisition to detect underground pipes. *NDT E Int.* **2017**, *91*, 22–31. [CrossRef]
71. Rasol, M.; Pais, J.C.; Pérez-Gracia, V.; Solla, M.; Fernandes, F.M.; Fontul, S.; Ayala-Cabrera, D.; Schmidt, F.; Assadollahi, H. GPR monitoring for road transport infrastructure: A systematic review and machine learning insights. *Constr. Build. Mater.* **2022**, *324*, 126686. [CrossRef]
72. Solla, M.; Pérez-Gracia, V.; Fontul, S. A Review of GPR Application on Transport Infrastructures: Troubleshooting and Best Practices. *Remote Sens.* **2021**, *13*, 672. [CrossRef]
73. Klewe, T.; Strangfeld, C.; Kruschwitz, S. Review of moisture measurements in civil engineering with Ground-Penetrating Radar—Applied methods and signal features. *Constr. Build. Mater.* **2021**, *278*, 122250. [CrossRef]
74. Tešić, K.; Baričević, A.; Serdar, M. Non-Destructive Corrosion Inspection of Reinforced Concrete Using Ground-Penetrating Radar: A Review. *Materials* **2021**, *14*, 975. [CrossRef]
75. Dabous, S.A.; Feroz, S. Condition monitoring of bridges with non-contact testing technologies. *Autom. Constr.* **2020**, *116*, 103224. [CrossRef]
76. Pajewski, L.; Fontul, S.; Solla, M. Chapter 10: Ground-Penetrating Radar for the evaluation and monitoring of transport infrastructures. In *Innovation in Near-Surface Geophysics. Instrumentation, Application, and Data Processing Methods*; Elsevier: Amsterdam, The Netherlands, 2019. [CrossRef]
77. Lai, W.W.-L.; Dérobert, X.; Annan, P. A review of Ground-Penetrating Radar application in civil engineering: A 30-year journey from Locating and Testing to Imaging and Diagnosis. *NDT E Int.* **2018**, *96*, 58–78. [CrossRef]
78. Bachiri, T.; Khamlichi, A.; Bezzazi, M. Bridge deck condition assessment by using GPR: A review. In Proceedings of the 1st International Conference on Non-Destructive Evaluation of Composite Structures (NDECS 2017), Tetouan, Morocco, 25 November 2017. [CrossRef]
79. Rehman, S.K.U.; Ibrahim, Z.; Memon, S.A.; Jameel, M. Nondestructive test methods for concrete bridges: A review. *Constr. Build. Mater.* **2016**, *107*, 58–86. [CrossRef]
80. Evans, R.D.; Frost, M.; Stonecliffe-Jones, M.; Dixon, N. A review of pavement assessment using Ground-Penetrating Radar (GPR). In Proceedings of the 12th International Conference Ground-Penetrating Radar, Birmingham, UK, 16–19 June 2008.
81. McCann, D.; Forde, M. Review of NDT methods in the assessment of concrete and masonry structures. *NDT E Int.* **2001**, *34*, 71–84. [CrossRef]
82. Martinho, E.; Dionísio, A. Main geophysical techniques used for non-destructive evaluation in cultural built heritage: A review. *J. Geophys. Eng.* **2014**, *11*, 053001. [CrossRef]
83. Viberg, A.; Trinks, I.; Lidén, K. A review of the use of geophysical archaeological prospection in Sweden. *Archaeol. Prospect.* **2011**, *18*, 43–56. [CrossRef]
84. Conyers, L.B. *Ground-Penetrating Radar for Archaeology. Geophysical Methods for Archaeology*; Altamira Press: Lanham, MD, USA, 2004; ISBN 9780759107724.

85. Goodman, D.; Piro, S. *GPR Remote Sensing in Archaeology, Geotechnologies and the Environment*; Springer: Berlin, Germany, 2013; Volume 9.
86. Trinks, I.; Johansson, B.; Gustafsson, J.; Emilsson, J.; Friborg, J.; Gustafsson, C.; Nissen, J.; Hinterleitner, A. Efficient, large-scale archaeological prospection using a true three-dimensional Ground-Penetrating Radar Array system. *Archaeol. Prospect.* **2010**, *17*, 175–186. [CrossRef]
87. Bornik, A.; Wallner, M.; Hinterleitner, A.; Verhoeven, G.J.J.; Neubauer, W. Integrated volume visualisation of archaeological Ground-Penetrating Radar data. In Proceedings of the 16th Eurographics Work on Graphics and Cultural Heritage, Vienna, Austria, 12–15 November 2018.
88. Löcker, K.; Baldwin, E.; Neubauer, W.; Gaffney, W.; Gaffney, C.; Hinterleitner, A.; Garwood, P.J.; Trinks, I.; Wallner, M. The Stonehenge hidden landscape project—Data acquisition, processing, interpretation. In Proceedings of the 10th International Conference Archaeological Prospection, Vienna, Austria, 20 May–2 June 2013.
89. Lazăr, C.; Ene, D.; Parnic, V.; Popovici, D.N.; Florea, M. Ground-Penetrating Radar prospections in Romania. Măriuta-la movilă necropolis, a case study. *Mediterr. Archaeol. Archaeom.* **2011**, *11*, 79–89.
90. Leucci, G.; De Giorgi, L.; Di Giacomo, G.; Ditaranto, I.; Miccoli, I.; Scardozzi, G. 3D GPR survey for the archaeological characterization of the ancient Messapian necropolis in Lecce, South Italy. *J. Archaeol. Sci. Rep.* **2016**, *7*, 290–302. [CrossRef]
91. Bornik, A.; Neubauer, W. 3D Visualization Techniques for Analysis and Archaeological Interpretation of GPR Data. *Remote Sens.* **2022**, *14*, 1709. [CrossRef]
92. Pérez-Gracia, V.; Caselles, J.O.; Clapés, J.; Martinez, G.; Osorio, R. Non-destructive analysis in cultural heritage buildings: Evaluating the Mallorca cathedral supporting structures. *NDT E Int.* **2013**, *59*, 40–47. [CrossRef]
93. Catapano, I.; Ludeno, G.; Soldovieri, F.; Tosti, F.; Padeletti, G. Structural assessment via Ground-Penetrating Radar at the Consoli Palace of Gubbio (Italy). *Remote Sens.* **2018**, *10*, 45. [CrossRef]
94. Fontul, S.; Solla, M.; Cruz, H.; Machado, J.S.; Pajewski, L. Ground-Penetrating Radar investigations in the Noble Hall of the São Carlos theater in Lisbon, Portugal. *Surv. Geophys.* **2018**, *39*, 1125–1147. [CrossRef]
95. Novo, A.; Lorenzo, H.; Rial, F.I.; Solla, M. Three-dimensional Ground-Penetrating Radar strategies over an indoor archaeological site: Convent of Santo Domingo (Lugo, Spain). *Archaeol. Prospect.* **2010**, *17*, 213–222. [CrossRef]
96. Leucci, G.; De Giorgi, L.; Ditaranto, I.; Miccoli, I.; Scardozzi, G. Ground-Penetrating Radar Prospections in Lecce Cathedral: New Data about the Crypt and the Structures under the Church. *Remote Sens.* **2021**, *13*, 1692. [CrossRef]
97. Masini, N.; Nuzzo, L.; Rizzo, E. GPR investigations for the study and the restoration of the Rose Window of Troia Cathedral (Southern Italy). *Near. Surf. Geophys.* **2007**, *5*, 287–300. [CrossRef]
98. Santos-Assunçao, S.; Dimitriadis, K.; Konstantakis, Y.; Perez-Gracia, V.; Anagnostopoulou, E.; Gonzalez-Drigo, R. Ground-Penetrating Radar evaluation of the ancient Mycenaean monument Tholos Acharnon tomb. *Near. Surface Geophys.* **2016**, *14*, 197–205. [CrossRef]
99. Kadioglu, S. Transparent 2d/3d half bird's-eye view of Ground-Penetrating Radar data set in archaeology and cultural heritage. In *Imaging and Radioanalytical Techniques in Interdisciplinary Research—Fundamentals and Cutting Edge Applications*; IntechOpen: London, UK, 2013.
100. Dimitriadis, K. GPR in the Preservation of Cultural Heritage. In *COST Action TU1208, Proceedings of the TU1208 Third General Meeting, London, UK, 4–6 March 2015*; Aracne, Ariccia: Rome, Italy, 2015; ISBN 978-88-548-8486-1.
101. Solla, M.; Riveiro, B.; Lorenzo, H.; Armesto, J. Ancient stone bridge surveying by Ground-Penetrating Radar and numerical modeling methods. *J. Bridge Eng.* **2014**, *19*, 110–119. [CrossRef]
102. Alani, A.M.; Tosti, F.; Bianchini Ciampoli, L.; Gagliardi, V.; Benedetto, A. An integrated investigative approach in health monitoring of masonry arch bridges using GPR and InSAR technologies. *NDT E Int.* **2020**, *115*, 102288. [CrossRef]
103. Lombardi, F.; Lualdi, M.; Garavaglia, E. Masonry texture reconstruction for building seismic assessment: Practical evaluation and potentials of Ground-Penetrating Radar methodology. *Constr. Build. Mater.* **2021**, *299*, 124189. [CrossRef]
104. Danese, M.; Sileo, M.; Masini, N. Geophysical Methods and Spatial Information for the Analysis of Decaying Frescoes. *Surv. Geophys.* **2018**, *39*, 1149–1166. [CrossRef]
105. Calia, A.; Lettieri, M.; Leucci, G.; Matera, L.; Persico, R.; Sileo, M. The mosaic of the crypt of St. Nicholas in Bari (Italy): Integrated GPR and laboratory diagnostic study. *J. Archaeol. Sci.* **2013**, *40*, 4162–4169. [CrossRef]
106. Caldeira, B.; Oliveira, R.J.; Teixidó, T.; Borges, J.F.; Henriques, R.; Carneiro, A.; Peña, J.A. Studying the Construction of Floor Mosaics in the Roman Villa of Pisões (Portugal) Using Noninvasive Methods: High-Resolution 3D GPR and Photogrammetry. *Remote Sens.* **2019**, *11*, 1882. [CrossRef]
107. Carrozzo, M.T.; Leucci, G.; Negri, S.; Pierri, C.; Varola, A. Ground-Penetrating Radar: Preliminary results to locate vertebrate fossils. In Proceedings of the SAGEEP 2003, Environ and Engineering Geophysical Society, San Antonio, TX, USA, 6–10 April 2003; pp. 1017–1103.
108. Tinelli, C.; Ribolini, A.; Bianucci, G.; Bini, M.; Landini, W. Ground-Penetrating Radar and palaeontology: The detection of sirenian fossil bones under a sunflower field in Tuscany (Italy). *C. R. Palevol* **2012**, *11*, 445–454. [CrossRef]
109. Main, D.J.; Hammon, W.S. The application of Ground-Penetrating Radar as a mapping technique at vertebrate fossil excavations in the Cretaceous of Texas. *Cretaceous Res.* **2003**, *24*, 335–345. [CrossRef]
110. Manataki, M.; Vafidis, A.; Sarris, A. GPR Data Interpretation Approaches in Archaeological Prospection. *Appl. Sci.* **2021**, *11*, 7531. [CrossRef]

111. Küçükdemirci, M.; Sarris, A. Deep learning based automated analysis of archaeo-geophysical images. *Archaeol. Prospect.* **2020**, *27*, 107–118. [CrossRef]
112. Puente, I.; Solla, M.; Lagüela, S.; Sanjurjo-Pinto, J. Reconstructing the Roman Site "*Aquis Querquennis*" (Bande, Spain) from GPR, T-LiDAR and IRT Data Fusion. *Remote Sens.* **2018**, *10*, 379. [CrossRef]
113. Núñez-Nieto, X.; Solla, M.; Novo, A.; Lorenzo, H. Three-dimensional Ground-Penetrating Radar methodologies for the characterization and volumetric reconstruction of underground tunneling. *Constr. Build. Mater.* **2014**, *71*, 551–560. [CrossRef]
114. Adamopoulos, E.; Rinaudo, F. Close-Range Sensing and Data Fusion for Built Heritage Inspection and Monitoring—A Review. *Remote Sens.* **2021**, *13*, 3936. [CrossRef]
115. Nuzzo, L.; Quarta, T. GPR prospecting of cylindrical structures in cultural heritage applications: A review of geometric issues. *Near Surf. Geophys.* **2012**, *10*, 17–34. [CrossRef]
116. Leucci, G. Nondestructive testing technologies for Cultural Heritage: Overview. In *Nondestructive Testing for Archaeology and Cultural Heritage. A Practical Guide and New Perspectives*; Springer: Cham, Switzerland, 2019.
117. Trinks, I.; Hinterleitner, A.; Neubauer, W.; Nau, E.; Löcker, K.; Wallner, M.; Gabler, M.; Filzwieser, R.; Wilding, J.; Schiel, H.; et al. Large-area high-resolution Ground-Penetrating Radar measurements for archaeological prospection. *Archaeol. Prospect.* **2018**, *25*, 171–195. [CrossRef]
118. Cuenca-García, C.; Risbøl, O.; Bates, C.; Stamnes, A.; Skoglund, F.; Ødegård, Ø.; Viberg, A.; Koivisto, S.; Fuglsang, M.; Gabler, M.; et al. Sensing Archaeology in the North: The Use of Non-Destructive Geophysical and Remote Sensing Methods in Archaeology in Scandinavian and North Atlantic Territories. *Remote Sens.* **2020**, *12*, 3102. [CrossRef]
119. Pajewski, L.; Solla, M.; Küçükdemirci, M. Ground-Penetrating Radar for Archaeology and Cultural-Heritage diagnostics: Activities Carried Out in COST Action TU1208. In *Nondestructive Techniques for the Assessment and Preservation of Historic Structures*; Gonçalves, L.M.S., Rodrigues, H., Gaspar, F., Eds.; CRC Press: Boca Raton, FL, USA, 2018.
120. Pérez-Gracia, V.; Fontul, S.; Santos-Assunçao, S.; Marecos, V. Geophysics: Fundamentals and Applications in Structures and Infrastructures. In *NDT for the Evaluation of Structures and Infrastructure*; Riveiro, B., Solla, M., Eds.; CRC Press/Balkema: Leiden, The Netherlands, 2016. [CrossRef]
121. Daniels, D.J. A review of GPR for landmine detection. *Sens. Imaging* **2006**, *7*, 90–123. [CrossRef]
122. Barone, P.M.; Di Maggio, R.M. Forensic geophysics: Ground-Penetrating Radar (GPR) techniques and missing persons investigations. *Forensic Sci. Res.* **2019**, *4*, 337–340. [CrossRef] [PubMed]
123. Elis, V.R.; Almeida, E.R.; Porsani, J.L.; Stangari, M.C. Ground-Penetrating Radar, resistivity, and induced polarization applied in forensic research in tropical soils. In Proceedings of the 18th International Conference on Ground-Penetrating Radar, Golden, Colorado, 14–19 June 2020. [CrossRef]
124. Barone, P.; Ferrara, C.; Pettinelli, E.; Annan, A.; Fazzari, A.; Redman, D. Forensic Geophysics: How GPR Could Help Police Investigations. In Proceedings of the Near Surface Geoscience 2012—18th European Meeting of Environmental and Engineering Geophysics, Paris, France, 3–5 September 2012; European Association of Geoscientists & Engineers: Houten, The Netherlands, 2012. [CrossRef]
125. Niessen, J.; Kliem, E.; Pöhlking, E.; Nick, K.P. The use of Ground-Penetrating Radar to search for persons buried by avalanches. In Proceedings of the Fifth International Conferention on Ground-Penetrating Radar, Kitchener, ON, Canada, 12–16 June 1994.
126. Novo, A.; Lorenzo, H.; Rial, F.I.; Solla, M. 3D GPR in forensics: Finding a clandestine grave in a mountainous environment. *Forensic Sci. Int.* **2011**, *204*, 134–138. [CrossRef] [PubMed]
127. Sato, M. Introduction of the advanced ALIS: Advanced landmine Imaging System. In *Detection and Sensing of Mines, Explosive Objects, and Obscured Targets XXIII*; SPIE: Cergy-Pontoise, France, 2018.
128. Sato, M. Disaster Monitoring by SAR, Gb-SAR and GPR. In Proceedings of the IGARSS 2019—2019 IEEE International Geoscience and Remote Sensing Symposium, Yokohama, Japan, 28 July–2 August 2019; pp. 4752–4755. [CrossRef]
129. Núñez-Nieto, X.; Solla, M.; Lorenzo, H. Applications of GPR for Humanitarian Assistance and Security. In *Civil Engineering Applications of Ground-Penetrating Radar*; Benedetto, A., Pajewski, L., Eds.; Springer Transactions in Civil and Environ Engineering; Springer: Cham, Switzerland, 2015. [CrossRef]
130. Ferrara, V. Technical survey about available technologies for detecting buried people under rubble or avalanches. *WIT Trans. Built Environ.* **2015**, *150*, 91–101. [CrossRef]
131. Cist, D.B. Non-destructive evaluation after destruction: Using Ground-Penetrating Radar for search and rescue. In Proceedings of the 7th International Symposium on Nondestructive Testing in Civil Engineering, Nantes, France, 30 June–3 July 2009.
132. Sovlukov, A.S.; Khablov, D.V. The capabilities of microwave methods for alive people detection through obstacles by breathing and heartbeat. *Autom. Remote Control* **2014**, *75*, 2060–2076. [CrossRef]
133. Van, N.T.P.; Tang, L.; Demir, V.; Hasan, S.F.; Minh, N.D.; Mukhopadhyay, S. Review-Microwave Radar Sensing Systems for Search and Rescue Purposes. *Sensors* **2019**, *19*, 2879. [CrossRef]
134. Instanes, A.; Lønne, I.; Sandaker, K. Location of avalanche victims with Ground-Penetrating Radar. *Cold Reg. Sci. Technol.* **2004**, *38*, 55–61. [CrossRef]
135. Olhoeft, G.R.; Modroo, J.J. Locating and identifying avalanche victims with GPR. *Lead. Edge* **2006**, *25*, 306–308. [CrossRef]
136. Diamanti, N.; Annan, A.P.; Giannakis, I. Predicting GPR performance for buried victim search & rescue. In Proceedings of the 16th International Conference on Ground-Penetrating Radar (GPR), Hong Kong, China, 13–16 June 2016.

137. Chen, J.; Li, S.; Liu, D.; Li, X. AiRobSim: Simulating a Multisensor Aerial Robot for Urban Search and Rescue Operation and Training. *Sensors* **2020**, *20*, 5223. [CrossRef]
138. Garcia-Fernandez, M.; Alvarez-Lopez, Y.; Las Heras, F. Autonomous Airborne 3D SAR Imaging System for Subsurface Sensing: UWB-GPR on Board a UAV for Landmine and IED Detection. *Remote Sens.* **2019**, *11*, 2357. [CrossRef]
139. Grazzini, G.; Pieraccini, M.; Parrini, F.; Spinetti, A.; Macaluso, G.; Dei, D.; Atzeni, C. An ultra-wideband high-dynamic range GPR for detecting buried people after collapse of buildings. In Proceedings of the XIII International Conference on Ground-Penetrating Radar, Lecce, Italy, 21–25 June 2010; pp. 1–6. [CrossRef]
140. Ivashchuk, V.E.; Prokhorenko, V.P.; Pitertsev, A.A.; Yanovsky, F.J. Through-the-wall moving target surveillance using GPR. In Proceedings of the 2013 European Microwave Conference, Nuremberg, Germany, 6–10 October 2013; pp. 1787–1790.
141. Li, J.; Liu, L.; Zeng, Z.; Liu, F. Advanced Signal Processing for Vital Sign Extraction With Applications in UWB Radar Detection of Trapped Victims in Complex Environments. *IEEE J. Sel. Top. Appl. Earth Obs. Remote Sens.* **2014**, *7*, 783–791. [CrossRef]
142. Yan, K.; Wu, S.; Fang, G. Detection of Quasi-Static Trapped Human Being Using Mono-Static UWB Life-Detection Radar. *Appl. Sci.* **2021**, *11*, 3129. [CrossRef]
143. Humanitarian Demining, Geneva International Centre for, "Guidebook on Detection Technologies and Systems for Humanitarian Demining". Global CWD Repository. 2006. Available online: https://commons.lib.jmu.edu/cisr-globalcwd/1301 (accessed on 3 May 2022).
144. Capineri, L.; Ivashov, S.; Bechtel, T.; Zhuravlev, A.; Falorni, P.; Windsor, C.; Sheyko, A. Comparison of GPR sensor types for landmine detection and classification. In Proceedings of the 12th International Conference Ground-Penetrating Radar, Birmingham, UK, 16–19 June 2008; Volume 55. No. 2008.
145. Van Verre, W.; Podd, F.J.; Tan, Y.M.; Gao, X.; Peyton, A.J. A Comparison of Solid and Loaded Bowtie Antennas in GPR for the Detection of Buried Landmines. In Proceedings of the 2018 17th International Conference Ground-Penetrating Radar (GPR), Rapperswil, Switzerland, 18–21 June 2018; pp. 1–6. [CrossRef]
146. Bestagini, P.; Lombardi, F.; Lualdi, M.; Picetti, F.; Tubaro, S. Landmine Detection Using Autoencoders on Multipolarization GPR Volumetric Data. *IEEE Trans. Geosci. Remote Sens.* **2020**, *59*, 182–195. [CrossRef]
147. Lombardi, F.; Griffiths, H.D.; Lualdi, M.; Balleri, A. Characterization of the Internal Structure of Landmines Using Ground-Penetrating Radar. *IEEE Geosci. Remote Sens. Lett.* **2020**, *18*, 266–270. [CrossRef]
148. Núñez-Nieto, X.; Solla, M.; Gómez-Pérez, P.; Lorenzo, H. GPR Signal Characterization for Automated Landmine and UXO Detection Based on Machine Learning Techniques. *Remote Sens.* **2014**, *6*, 9729–9748. [CrossRef]
149. Lombardi, F.; Lualdi, M.; Picetti, F.; Bestagini, P. Identification and Recognition of Landmine Internal Structure Scattering Contribution from GPR Data. In Proceedings of the 25th European Meeting of Environmental and Engineering Geophysics, Hague, The Netherlands, 8–12 September 2019.
150. Kumlu, D.; Erer, I. Clutter removal techniques in Ground-Penetrating Radar for landmine detection: A Survey. In *Operations Research for Military Organizations*; IGI Global: Hershey, PA, USA, 2019; pp. 375–399. [CrossRef]
151. Hibbard, M.W.; Etebari, A. NIITEK-NVESD AMDS program and interim field-ready system. In Proceedings of the SPIE Detection and Sensing of Mines, Explosive Objects, and Obscured Targets XV, Orlando, FL, USA, 5–9 April 2010; SPIE: Bellingham, WA, USA, 2010; Volume 7664, p. 766413. [CrossRef]
152. Rubio-Melendi, D.; Gonzalez-Quirós, A.; Roberts, D.; García, M.D.C.G.; Domínguez, A.C.; Pringle, J.K.; Fernández-Álvarez, J.-P. GPR and ERT detection and characterization of a mass burial, Spanish Civil War, Northern Spain. *Forensic Sci. Int.* **2018**, *287*, e1–e9. [CrossRef]
153. Hansen, J.D.; Pringle, J.K.; Goodwin, J. GPR and bulk ground resistivity surveys in graveyards: Locating unmarked burials in contrasting soil types. *Forensic Sci. Int.* **2014**, *237*, e14–e29. [CrossRef]
154. Fiedler, S.; Illich, B.; Berger, J.; Graw, M. The effectiveness of Ground-Penetrating Radar surveys in the location of unmarked burial sites in modern cemeteries. *J. Appl. Geophys.* **2009**, *68*, 380–385. [CrossRef]
155. Kelly, T.; Angel, M.; O'Connor, D.; Huff, C.; Morris, L.; Wach, G. A novel approach to 3D modelling Ground-Penetrating Radar (GPR) data—A case study of a cemetery and applications for criminal investigation. *Forensic Sci. Int.* **2021**, *325*, 110882. [CrossRef]
156. Berezowski, V.; Mallett, X.; Ellis, J.; Moffat, I. Using Ground-Penetrating Radar and Resistivity Methods to Locate Unmarked Graves: A Review. *Remote Sens.* **2021**, *13*, 2880. [CrossRef]
157. Giovanneschi, F.; Mishra, K.V.; Gonzalez-Huici, M.A.; Eldar, Y.C.; Ender, J.H.G. Dictionary Learning for Adaptive GPR Landmine Classification. *IEEE Trans. Geosci. Remote Sens.* **2019**, *57*, 10036–10055. [CrossRef]
158. Barkataki, N.; Tiru, B.; Sarma, U. A CNN model for predicting size of buried objects from GPR B-Scans. *J. Appl. Geophys.* **2022**, *200*, 104620. [CrossRef]
159. Moalla, M.; Frigui, H.; Karem, A.; Bouzid, A. Application of Convolutional and Recurrent Neural Networks for Buried Threat Detection Using Ground-Penetrating Radar Data. *IEEE Trans. Geosci. Remote Sens.* **2020**, *58*, 7022–7034. [CrossRef]
160. Temlioglu, E.; Erer, I. A Novel Convolutional Autoencoder-Based Clutter Removal Method for Buried Threat Detection in Ground-Penetrating Radar. *IEEE Trans. Geosci. Remote Sens.* **2021**, *60*, 1–13. [CrossRef]
161. Bralich, J.; Reichman, D.; Collins, L.M.; Malof, J.M. Improving convolutional neural networks for buried target detection in Ground-Penetrating Radar using transfer learning via pretraining. In Proceedings of the SPIE Detection and Sensing of Mines, Explosive Objects, and Obscured Targets XXII, Anaheim, CA, USA, 9–13 April 2017; SPIE: Bellingham, WA, USA, 2017; Volume 10182, pp. 198–208. [CrossRef]

162. Hu, D.; Chen, J.; Li, S. Reconstructing unseen spaces in collapsed structures for search and rescue via deep learning based radargram inversion. *Autom. Constr.* **2022**, *140*, 104380. [CrossRef]
163. Wood, A.; Wood, R.; Charnley, M. Through-the-wall radar detection using machine learning. *Results Appl. Math.* **2020**, *7*, 100106. [CrossRef]
164. Brito-Da-Costa, A.M.; Martins, D.; Rodrigues, D.; Fernandes, L.; Moura, R.; Madureira-Carvalho, A. Ground-Penetrating Radar for Buried Explosive Devices Detection: A Case Studies Review. *Aust. J. Forensic Sci.* **2021**, 1–20. [CrossRef]
165. Pochanin, G.; Capineri, L.; Bechtel, T.; Ruban, V.; Falorni, P.; Crawford, F.; Ogurtsova, T.; Bossi, L. Radar Systems for Landmine Detection: Invited Paper. In Proceedings of the 2020 IEEE Ukrainian Microwave Week (UkrMW), Kharkiv, Ukraine, 21–25 September 2020; pp. 1118–1122. [CrossRef]
166. Tellez, O.L.L.; Scheers, B. Ground-Penetrating Radar for Close-in Mine Detection. In *Mine Action, The Research Experience of the Royal Military Academy of Belgium*; IntechOpen: London, UK, 2017. [CrossRef]
167. Crocco, L.; Ferrara, V. A review on Ground-Penetrating Radar technology for the detection of buried or trapped victims. In Proceedings of the 2014 International Conference Collaboration Technologies and Systems (CTS), Minneapolis, MN, USA, 19–23 May 2014; pp. 535–540.
168. Sujatmiko, W.; Prastio, R.P.; Danudirdjo, D.; Suksmono, A.B. A Review of Radars to Detect Survivors Buried Under Earthquake Rubble. In Proceedings of the 2017 5th International Conference Instrumentation, Communications, Information Technology, and Biomedical Engineering (ICICI-BME), Bandung, Indonesia, 6–7 November 2017; pp. 309–313.
169. Schultz, J.J. *The Application of Ground-Penetrating Radar for Forensic Grave Detection. A Companion to Forensic Anthropology*; Wiley: Hoboken, NJ, USA, 2012; pp. 85–100. [CrossRef]
170. Leucci, G. *Forensic Geosciences and Geophysics: Overview. Advances in Geophysical Methods Applied to Forensic Investigations*; Springer: Cham, Switzerland, 2020; pp. 11–48. [CrossRef]
171. Drahor, M.G.; Berge, M.A.; Öztürk, C. Integrated geophysical surveys for the subsurface mapping of buried structures under and surrounding of the Agios Voukolos Church in İzmir, Turkey. *J. Archaeol. Sci.* **2011**, *38*, 2231–2242. [CrossRef]
172. Fritzsche, M.; Löhlein, O. Sensor Fusion for the Detection of Landmines. *Subsurf. Sens. Technol. Appl.* **2000**, *1*, 247–267. [CrossRef]
173. Arosio, D. A microseismic approach to locate survivors trapped under rubble. *Near Surf. Geophys.* **2010**, *8*, 623–633. [CrossRef]
174. Peters, L.P.; Daniels, J.J.; Young, J.D. Ground-Penetrating Radar as a subsurface environmental sensing tool. *Proc. IEEE* **1994**, *82*, 1802–1822. [CrossRef]
175. Vereecken, H.; Binley, A.; Cassiani, G.; Revil, A.; Titov, K. (Eds.) *Applied Hydrogeophysics*; NATO Science Series; Springer: Dordrecht, The Netherlands, 2006; Volume 71. [CrossRef]
176. Hubbard, S.; Chen, J.; Williams, K.; Rubin, Y.; Peterson, J. Environmental and agricultural applications of GPR. In Proceedings of the 3rd International Work on Advanced Ground-Penetrating Radar—IWAGPR 2005, Delft, The Netherlands, 2–3 May 2005.
177. Alcalá, F.J.; Paz, M.C.; Martínez-Pagán, P.; Santos, F.M. Integrated Geophysical Methods for Shallow Aquifers Characterization and Modelling. *Appl. Sci.* **2022**, *12*, 2271. [CrossRef]
178. Irving, J.; Xu, Z.; Lindsay, K.M.; Bradford, J.; Zhu, P.; Holliger, K. Determination of the correlation structure of an alluvial aquifer from multi-frequency 3D GPR reflection measurements. *AGU Fall Meet. Abstr.* **2019**, *2019*, H43F-2040.
179. Kowalsky, M.B.; Finsterle, S.; Peterson, J.; Hubbard, S.; Rubin, Y.; Majer, E.; Ward, A.; Gee, G. Estimation of field-scale soil hydraulic and dielectric parameters through joint inversion of GPR and hydrological data. *Water Resour. Res.* **2005**, *41*, W11425. [CrossRef]
180. Bowling, J.C.; Rodriguez, A.B.; Harry, D.L.; Zheng, C. Delineating Alluvial Aquifer Heterogeneity Using Resistivity and GPR Data. *Ground Water* **2005**, *43*, 890–903. [CrossRef]
181. Montgomery, L.; Miège, C.; Miller, J.; Scambos, T.A.; Wallin, B.; Miller, O.; Solomon, D.K.; Forster, R.; Koenig, L. Hydrologic Properties of a Highly Permeable Firn Aquifer in the Wilkins Ice Shelf, Antarctica. *Geophys. Res. Lett.* **2020**, *47*, e2020GL089552. [CrossRef]
182. Chen, J.; Hubbard, S.; Rubin, Y. Estimating the hydraulic conductivity at the south oyster site from geophysical tomographic data using Bayesian Techniques based on the normal linear regression model. *Water Resour. Res.* **2001**, *37*, 1603–1613. [CrossRef]
183. Lunt, I.; Hubbard, S.; Rubin, Y. Soil moisture content estimation using Ground-Penetrating Radar reflection data. *J. Hydrol.* **2005**, *307*, 254–269. [CrossRef]
184. Turesson, A. Water content and porosity estimated from Ground-Penetrating Radar and resistivity. *J. App. Geophys.* **2016**, *58*, 99–111. [CrossRef]
185. Klotzsche, A.; Jonard, F.; Looms, M.; van der Kruk, J.; Huisman, J. Measuring Soil Water Content with Ground-Penetrating Radar: A Decade of Progress. *Vadose Zone J.* **2018**, *17*, 180052–180059. [CrossRef]
186. Grote, K.; Leverett, K. Comparison of pedotransfer functions for high-resolution mapping of hydraulic conductivity in agricultural soils using GPR. *AGU Fall Meet. Abstr.* **2019**, *2019*, NS31A-0766.
187. Steelman, C.M.; Endres, A.L. Comparison of Petrophysical Relationships for Soil Moisture Estimation using GPR Ground Waves. *Vadose Zone J.* **2011**, *10*, 270–285. [CrossRef]
188. Shokri, M.; Gao, Y.; Kibler, K.M.; Wang, D.; Wightman, M.J.; Rice, N. Contaminant transport from stormwater management areas to a freshwater karst spring in Florida: Results of near-surface geophysical investigations and tracer experiments. *J. Hydrol. Reg. Stud.* **2022**, *40*, 101055. [CrossRef]

189. Fuente, J.V. Detection and Delineating of Hydrocarbon Contaminants by Using Time and Frequency Analysis of Ground-Penetrating Radar. *J. Geosci. Environ. Prot.* **2021**, *09*, 35–56. [CrossRef]
190. Busch, S.; van der Kruk, J.; Vereecken, H. Improved Characterization of Fine-Texture Soils Using On-Ground GPR Full-Waveform Inversion. *IEEE Trans. Geosci. Remote Sens.* **2013**, *52*, 3947–3958. [CrossRef]
191. Zajc, M.; Urbanc, J.; Pečan, U.; Glavan, M.; Pintar, M. Using 3D GPR for determining soil conditions in precision agriculture. In Proceedings of the 18th International Conference on Ground-Penetrating Radar, Golden, CO, USA, 14–19 June 2020; pp. 291–294.
192. Lombardi, F.; Lualdi, M. Step-Frequency Ground-Penetrating Radar for Agricultural Soil Morphology Characterisation. *Remote Sens.* **2019**, *11*, 1075. [CrossRef]
193. Kiełbasa, P.; Zagórda, M.; Juliszewski, T.; Akinsunmade, A.; Tomecka, S.; Karczewski, J.; Pysz, P. Assessment of the possibility of using GPR to determine the working resistance force of tools for subsoil reclamation. *J. Phys. Conf. Ser.* **2021**, *1782*, 012013. [CrossRef]
194. Alani, A.M.; Lantini, L. Recent Advances in Tree Root Mapping and Assessment Using Non-destructive Testing Methods: A Focus on Ground-Penetrating Radar. *Surv. Geophys.* **2019**, *41*, 605–646. [CrossRef]
195. Knight, R. Ground-Penetrating Radar for Environmental Applications. *Annu. Rev. Earth Planet. Sci.* **2001**, *29*, 229–255. [CrossRef]
196. Urbini, S.; Baskaradas, J.A. GPR as an Effective Tool for Safety and Glacier Characterization: Experiences and Future Development. In Proceedings of the XIII Internarional Conference on Ground-Penetrating Radar, Lecce, Italy, 21–25 June 2010; pp. 1–6. [CrossRef]
197. Francke, J.; Dobrovolskiy, A. Challenges and opportunities with drone-mounted GPR. In Proceedings of the First Int Meeting for Applied Geoscience & Energy, Online, 26 September–1 October 2021; pp. 3043–3047.
198. Forte, E.; Bondini, M.B.; Bortoletto, A.; Dossi, M.; Colucci, R.R. Pros and Cons in Helicopter-Borne GPR Data Acquisition on Rugged Mountainous Areas: Critical Analysis and Practical Guidelines. *Pure Appl. Geophys.* **2019**, *176*, 4533–4554. [CrossRef]
199. Forte, E.; Santin, I.; Ponti, S.; Colucci, R.; Gutgesell, P.; Guglielmin, M. New insights in glaciers characterization by differential diagnosis integrating GPR and remote sensing techniques: A case study for the Eastern Gran Zebrù glacier (Central Alps). *Remote Sens. Environ.* **2021**, *267*, 112715. [CrossRef]
200. Santin, I.; Colucci, R.; Žebre, M.; Pavan, M.; Cagnati, A.; Forte, E. Recent evolution of Marmolada glacier (Dolomites, Italy) by means of ground and airborne GPR surveys. *Remote Sens. Environ.* **2019**, *235*, 111442. [CrossRef]
201. Stubbs, E.F.; Nobes, D.C. Dynamics of the folds of the McMurdo Ice Shelf, Scott Base, Antarctica. In Proceedings of the 2018 17th International Conference Ground-Penetrating Radar (GPR), Rapperswil, Switzerland, 18–21 June 2018; pp. 1–6. [CrossRef]
202. Di Paolo, F.; Cosciotti, B.; Lauro, S.E.; Mattei, E.; Pettinelli, E. A critical analysis on the uncertainty computation in Ground-Penetrating Radar-retrieved dry snow parameters. *Geophysics* **2020**, *85*, H39–H49. [CrossRef]
203. Giese, A.; Arcone, S.; Hawley, R.; Lewis, G.; Wagnon, P. Detecting supraglacial debris thickness with GPR under suboptimal conditions. *J. Glaciol.* **2021**, *67*, 1108–1120. [CrossRef]
204. Grab, M.; Mattea, E.; Bauder, A.; Huss, M.; Rabenstein, L.; Hodel, E.; Linsbauer, A.; Langhammer, L.; Schmid, L.; Church, G.; et al. Ice thickness distribution of all Swiss glaciers based on extended Ground-Penetrating Radar data and glaciological modeling. *J. Glaciol.* **2021**, *67*, 1074–1092. [CrossRef]
205. Forte, E.; Santin, I.; Colucci, R.R.; Dossi, M.; Guglielmin, M.; Pipan, M.; Roncoroni, G.; Žebre, M. GPR data analysis for cold and warm ice detection and characterization in polythermal glaciers. In Proceedings of the 18th International Conference on Ground-Penetrating Radar, Golden, CO, USA, 14–19 June 2020.
206. Delf, R.; Bingham, R.G.; Curtis, A.; Singh, S.; Giannopoulos, A.; Schwarz, B.; Borstad, C.P. Reanalysis of Polythermal Glacier Thermal Structure Using Radar Diffraction Focusing. *J. Geophys. Res. Earth Surf.* **2022**, *127*, e2021JF006382. [CrossRef]
207. Kunz, J.; Kneisel, C. Glacier–Permafrost Interaction at a Thrust Moraine Complex in the Glacier Forefield Muragl, Swiss Alps. *Geosciences* **2020**, *10*, 205. [CrossRef]
208. Shen, Y.; Zuo, R.; Liu, J.; Tian, Y.; Wang, Q. Characterization and evaluation of permafrost thawing using GPR attributes in the Qinghai-Tibet Plateau. *Cold Reg. Sci. Technol.* **2018**, *151*, 302–313. [CrossRef]
209. Sudakova, M.; Sadurtdinov, M.; Skvortsov, A.; Tsarev, A.; Malkova, G.; Molokitina, N.; Romanovsky, V. Using Ground-Penetrating Radar for Permafrost Monitoring from 2015–2017 at CALM Sites in the Pechora River Delta. *Remote Sens.* **2021**, *13*, 3271. [CrossRef]
210. Pirot, G.; Huber, E.; Irving, J.; Linde, N. A Quantitative Comparison of GPR Sections to Reduce Geological Prior Uncertainty. In Proceedings of the 24th European Meeting of Environmental and Engineering Geophysics, Porto, Portugal, 9–12 September 2018; Volume 2018, pp. 1–5.
211. Francke, J.; Yelf, R. Applications of GPR for surface mining. In Proceedings of the 2nd International Workshop on Advanced Ground-Penetrating Radar, Delft, The Netherlands, 14–16 May 2003; pp. 115–119. [CrossRef]
212. Francke, J.; Utsi, V. Advances in long-range GPR systems and their applications to mineral exploration, geotechnical and static correction problems. *First Break* **2009**, *27*. [CrossRef]
213. Rezaei, A.; Hassani, H.; Moarefvand, P.; Golmohammadi, A. Determination of unstable tectonic zones in C–North deposit, Sangan, NE Iran using GPR method: Importance of structural geology. *J. Min. Environ.* **2019**, *10*, 177–195. [CrossRef]
214. Golosinski, T.S. (Ed.) *Mining in the New Millennium-Challenges and Opportunities*; CRC Press: Boca Raton, FL, USA, 2020. [CrossRef]
215. Liu, X.; Guo, L.; Cui, X.; Butnor, J.R.; Boyer, E.W.; Yang, D.; Chen, J.; Fan, B. An Automatic Processing Framework for In Situ Determination of Ecohydrological Root Water Content by Ground-Penetrating Radar. *IEEE Trans. Geosci. Remote Sens.* **2021**, *60*, 1–15. [CrossRef]

216. Zheng, J.; Teng, X.; Liu, J.; Qiao, X. Convolutional Neural Networks for Water Content Classification and Prediction with Ground-Penetrating Radar. *IEEE Access* **2019**, *7*, 185385–185392. [CrossRef]
217. Cui, F.; Ni, J.; Du, Y.; Zhao, Y.; Zhou, Y. Soil water content estimation using Ground-Penetrating Radar data via group intelligence optimization algorithms: An application in the Northern Shaanxi Coal Mining Area. *Energy Explor. Exploit.* **2020**, *39*, 318–335. [CrossRef]
218. Williams, R.M.; Ray, L.; Lever, J.H.; Burzynski, A.M. Crevasse Detection in Ice Sheets Using Ground-Penetrating Radar and Machine Learning. *IEEE J. Sel. Top. Appl. Earth Obs. Remote Sens.* **2014**, *7*, 4836–4848. [CrossRef]
219. Paz, C.; Alcalá, F.J.; Carvalho, J.M.; Ribeiro, L. Current uses of Ground-Penetrating Radar in groundwater-dependent ecosystems research. *Sci. Total Environ.* **2017**, *595*, 868–885. [CrossRef]
220. Zajícová, K.; Chuman, T. Application of Ground-Penetrating Radar methods in soil studies: A review. *Geoderma* **2019**, *343*, 116–129. [CrossRef]
221. Liu, X.; Dong, X.; Leskovar, D.I. Ground-Penetrating Radar for underground sensing in agriculture: A review. *Int. Agrophys.* **2016**, *30*, 533–543. [CrossRef]
222. Schroeder, D.M.; Bingham, R.G.; Blankenship, D.D.; Christianson, K.; Eisen, O.; Flowers, G.E.; Karlsson, N.B.; Koutnik, M.R.; Paden, J.D.; Siegert, M.J. Five decades of radioglaciology. *Ann. Glaciol.* **2020**, *61*, 1–13. [CrossRef]
223. Francke, J. A review of selected Ground-Penetrating Radar applications to mineral resource evaluations. *J. Appl. Geophys.* **2012**, *81*, 29–37. [CrossRef]
224. Guo, L.; Chen, J.; Cui, X.; Fan, B.; Lin, H. Application of Ground-Penetrating Radar for coarse root detection and quantification: A review. *Plant Soil* **2012**, *362*, 1–23. [CrossRef]
225. Riese, F.M.; Keller, S. Fusion of hyper spectral and Ground-Penetrating Radar data to estimate soil moisture. In Proceedings of the 2018 9th Workshop on Hyperspectral Image and Signal Processing: Evolution in Remote Sensing (WHISPERS), Amsterdam, The Netherlands, 23–26 September 2018; pp. 1–5. [CrossRef]
226. Capozzoli, L.; Giampaolo, V.; De Martino, G.; Perciante, F.; Lapenna, V.; Rizzo, E. ERT and GPR Prospecting Applied to Unsaturated and Subwater Analogue Archaeological Site in a Full Scale Laboratory. *Appl. Sci.* **2022**, *12*, 1126. [CrossRef]
227. Czaja, K. Applications of Data Fusion for Estimating Water Saturation at the Basis of Seismic, GPR and Resistivity Methods. In Proceedings of the 24th European Meeting of Environmental and Engineering Geophysics, Porto, Portugal, 9–12 September 2018; pp. 1–5. [CrossRef]
228. Butt, N.A.; Khan, M.Y.; Khattak, S.A.; Akhter, G.; Ge, Y.; Shah, M.T.; Farid, A. Geophysical and Geochemical Characterization of Solidwaste Dumpsite: A Case Study of Chowa Gujar, Peshawar (Part of Indus Basin). *Sustainability* **2022**, *14*, 1443. [CrossRef]
229. Wang, T.-P.; Chen, C.-C.; Tong, L.-T.; Chang, P.-Y.; Chen, Y.-C.; Dong, T.-H.; Liu, H.-C.; Lin, C.-P.; Yang, K.-H.; Ho, C.-J.; et al. Applying FDEM, ERT and GPR at a site with soil contamination: A case study. *J. Appl. Geophys.* **2015**, *121*, 21–30. [CrossRef]
230. Bristow, C.S.; Jol, H.M. An introduction to Ground-Penetrating Radar (GPR) in sediments. *Geol. Soc. Lond. Spec. Publ.* **2003**, *211*, 1–7. [CrossRef]
231. Jol, H.M.; Bristow, C.S. GPR in sediments: Advice on data collection, basic processing and interpretation, a good practice guide. *Geol. Soc. Lond. Spec. Publ.* **2003**, *211*, 9–27. [CrossRef]
232. Pipan, M.; Forte, E.; Moro, G.D.; Sugan, M.; Finetti, I. Multifold Ground-Penetrating Radar and resistivity to study the stratigraphy of shallow unconsolidated sediments. *Lead. Edge* **2003**, *22*, 876–881. [CrossRef]
233. Salinas Naval, V.; Santos-Assunçao, S.; Pérez-Gracia, V. GPR Clutter Amplitude Processing to Detect Shallow Geological Targets. *Remote. Sens.* **2018**, *10*, 88. [CrossRef]
234. Grasmück, M.; Green, A.G. 3-D Georadar Mapping: Looking Into the Subsurface. *Environ. Eng. Geosci.* **1996**, *II*, 195–200. [CrossRef]
235. Beres, M.; Green, A.; Huggenberger, P.; Horstmeyer, H. Mapping the architecture of glaciofluvial sediments with three-dimensional georadar. *Geology* **1995**, *23*, 1087–1090. [CrossRef]
236. Caselle, C.; Bonetto, S.; Comina, C.; Stocco, S. GPR surveys for the prevention of karst risk in underground gypsum quarries. *Tunn. Undergr. Space Technol.* **2019**, *95*, 103137. [CrossRef]
237. McClymont, A.F.; Green, A.G.; Streich, R.; Horstmeyer, H.; Tronicke, J.; Nobes, D.C.; Pettinga, J.; Campbell, J.; Langridge, R. Visualization of active faults using geometric attributes of 3D GPR data: An example from the Alpine Fault Zone, New Zealand. *Geophysics* **2008**, *73*, B11–B23. [CrossRef]
238. Liner, C.L.; Liner, J.L. Application of GPR to a site investigation involving shallow faults. *Lead. Edge* **1997**, *16*, 1649–1651. [CrossRef]
239. Lu, G.; Zhao, W.; Forte, E.; Tian, G.; Li, Y.; Pipan, M. Multi-frequency and multi-attribute GPR data fusion based on 2-D wavelet transform. *Measurement* **2020**, *166*, 108243. [CrossRef]
240. Noori, M.; Hassani, H.; Javaherian, A.; Amindavar, H.; Torabi, S. Automatic fault detection in seismic data using Gaussian process regression. *J. Appl. Geophys.* **2019**, *163*, 117–131. [CrossRef]
241. Zanzi, L.; Hojat, A.; Ranjbar, H.; Karimi-Nasab, S.; Azadi, A.; Arosio, D. GPR measurements to detect major discontinuities at Cheshmeh-Shirdoosh limestone quarry, Iran. *Bull. Eng. Geol. Environ.* **2017**, *78*, 743–752. [CrossRef]
242. Elkarmoty, M.; Tinti, F.; Kasmaeeyazdi, S.; Bonduà, S.; Bruno, R. 3D modeling of discontinuities using GPR in a commercial size ornamental limestone block. *Constr. Build. Mater.* **2018**, *166*, 81–86. [CrossRef]

243. Elkarmoty, M.; Tinti, F.; Kasmaeeyazdi, S.; Giannino, F.; Bonduà, S.; Bruno, R. Implementation of a Fracture Modeling Strategy Based on Georadar Survey in a Large Area of Limestone Quarry Bench. *Geosciences* **2018**, *8*, 481. [CrossRef]
244. Lombardi, F.; Lualdi, M. Multi-Azimuth Ground-Penetrating Radar Surveys to Improve the Imaging of Complex Fractures. *Geosciences* **2018**, *8*, 425. [CrossRef]
245. Molron, J.; Linde, N.; Baron, L.; Selroos, J.-O.; Darcel, C.; Davy, P. Which fractures are imaged with Ground-Penetrating Radar? Results from an experiment in the Äspö Hardrock Laboratory, Sweden. *Eng. Geol.* **2020**, *273*, 105674. [CrossRef]
246. Jeannin, M.; Garambois, S.; Grégoire, C.; Jongmans, D. Multiconfiguration GPR measurements for geometric fracture characterization in limestone cliffs (Alps). *Geophysics* **2006**, *71*, B85–B92. [CrossRef]
247. Conti, I.M.M.; de Castro, D.L.; Bezerra, F.H.R.; Cazarin, C.L. Porosity Estimation and Geometric Characterization of Fractured and Karstified Carbonate Rocks Using GPR Data in the Salitre Formation, Brazil. *Pure Appl. Geophys.* **2018**, *176*, 1673–1689. [CrossRef]
248. Giertzuch, P.-L.; Doetsch, J.; Kittila, A.; Jalali, M.; Schmelzbach, C.; Maurer, H.; Shakas, A. Monitoring salt tracer transport in granite rock using Ground-Penetrating Radar reflection imaging. In Proceedings of the 2018 17th International Conference on Ground-Penetrating Radar (GPR), Rapperswil, Switzerland, 18–21 June 2018; pp. 1–6. [CrossRef]
249. Doetsch, J.; Krietsch, H.; Schmelzbach, C.; Jalali, M.; Gischig, V.; Villiger, L.; Amann, F.; Maurer, H. Characterizing a decametre-scale granitic reservoir using Ground-Penetrating Radar and seismic methods. *Solid Earth* **2020**, *11*, 1441–1455. [CrossRef]
250. Gischig, V.S.; Giardini, D.; Amann, F.; Hertrich, M.; Krietsch, H.; Loew, S.; Maurer, H.; Villiger, L.; Wiemer, S.; Bethmann, F.; et al. Hydraulic stimulation and fluid circulation experiments in underground laboratories: Stepping up the scale towards engineered geothermal systems. *Géoméch. Energy Environ.* **2019**, *24*, 100175. [CrossRef]
251. Stove, G.; Robinson, M. New method for monitoring steam injection for Enhanced Oil Recovery (EOR) and for finding sources of geothermal heat. *ASEG Ext. Abstr.* **2018**, *2018*, 1–8. [CrossRef]
252. Solla, M.; Blázquez, C.S.; Nieto, I.M.; Rodríguez, J.L.; Maté-González, M. GPR Application on Geothermal Studies: The Case Study of the Thermal Baths of San Xusto (Pontevedra, Spain). *Remote Sens.* **2022**, *14*, 2667. [CrossRef]
253. Ribolini, A.; Bertoni, D.; Bini, M.; Sarti, G. Ground-Penetrating Radar Prospections to Image the Inner Structure of Coastal Dunes at Sites Characterized by Erosion and Accretion (Northern Tuscany, Italy). *Appl. Sci.* **2021**, *11*, 11260. [CrossRef]
254. Harari, Z. Ground-Penetrating Radar (GPR) for imaging stratigraphic features and groundwater in sand dunes. *J. Appl. Geophys.* **1996**, *36*, 43–52. [CrossRef]
255. Rees-Hughes, L.; Barlow, N.L.M.; Booth, A.D.; West, L.J.; Tuckwell, G.; Grossey, T. Unveiling buried aeolian landscapes: Reconstructing a late Holocene dune environment using 3D ground-penetrating radar. *J. Quat. Sci.* **2021**, *36*, 377–390. [CrossRef]
256. Bristow, C.; Pugh, J.; Goodall, T. Internal structure of aeolian dunes in Abu Dhabi determined using Ground-Penetrating Radar. *Sedimentology* **1996**, *43*, 995–1003. [CrossRef]
257. Schenk, C.J.; Gautier, D.L.; Olhoeft, G.R.; Lucius, J.E. Internal Structure of an Aeolian Dune using Ground-Penetrating Radar. *Aeolian Sediments Anc. Mod.* **1993**, 61–69. [CrossRef]
258. Guillemoteau, J.; Dujardin, J.-R.; Bano, M. Influence of grain size, shape and compaction on georadar waves: Examples of aeolian dunes. *Geophys. J. Int.* **2012**, *190*, 1455–1463. [CrossRef]
259. Moorman, B.J. Ground-Penetrating Radar Applications in Paleolimnology. In *Tracking Environ Change Using Lake Sediments*; Springer: Dordrecht, The Netherlands, 2005. [CrossRef]
260. Lorenzo, H.; Solla, M. Feasibility of the GPR Technique for the bathymetry and sub-bottom stratigraphy of a lake environment. *Geophys. Res. Abstr.* **2019**, *21*, EGU2019-14106.
261. Switzer, A.D.; Gouramanis, C.; Bristow, C.S.; Simms, A.R. Ground-Penetrating Radar (GPR) in coastal hazard studies. In *Geological Records of Tsunamis and other Extreme Waves*; Elsevier: Amsterdam, The Netherlands, 2020. [CrossRef]
262. Ryazantsev, P.; Rodionov, A.; Subetto, D. Waterborne GPR mapping of stratigraphic boundaries and turbidite sediments beneath the bottom of Lake Polevskoye, Karelia, NW Russia. *J. Paleolimnol.* **2021**, *66*, 261–277. [CrossRef]
263. Arcone, S.A. Sedimentary architecture beneath lakes subjected to storms: Control by turbidity current bypass and turbidite armouring, interpreted from ground-penetrating radar images. *Sedimentology* **2017**, *65*, 1413–1446. [CrossRef]
264. Bristow, C.; Buck, L. GPR Survey of Storegga Tsunami Deposits, Shetland Islands UK, and Geohazard Discussion. In *Engineering and Mining Geophysics*; European Association of Geoscientists & Engineers: Houten, The Netherlands, 2021; Volume 2021, pp. 1–8. [CrossRef]
265. Sambuelli, L.; Bava, S. Case study: A GPR survey on a morainic lake in northern Italy for bathymetry, water volume and sediment characterization. *J. Appl. Geophys.* **2012**, *81*, 48–56. [CrossRef]
266. Nesbitt, I.M.; Campbell, S.W.; Arcone, S.A.; Smith, S.M. Using Ground-Penetrating Radar and sidescan sonar to compare lake bottom geology in New England. *AGU Fall Meet. Abstr.* **2017**, *2017*, PP44B-01.
267. Buynevich, I.V.; Fitzgerald, D.M. High-Resolution Subsurface (GPR) Imaging and Sedimentology of Coastal Ponds, Maine, U.S.A.: Implications for Holocene Back-Barrier Evolution. *J. Sediment. Res.* **2003**, *73*, 559–571. [CrossRef]
268. Yao, X.; Liu, S.; Sun, M.; Wei, J.; Guo, W. Volume calculation and analysis of the changes in moraine-dammed lakes in the north Himalaya: A case study of Longbasaba lake. *J. Glaciol.* **2012**, *58*, 753–760. [CrossRef]
269. Lachhab, A.; Booterbaugh, A.; Beren, M. Bathymetry and Sediment Accumulation of Walker Lake, PA Using Two GPR Antennas in a New Integrated Method. *J. Environ. Eng. Geophys.* **2015**, *20*, 245–255. [CrossRef]
270. Rodionov, A.; Ryazantsev, P. GPR study of sapropel deposits in Karelian shallow water areas. In Proceedings of the 2018 17th International Conference Ground-Penetrating Radar (GPR), Rapperswil, Switzerland, 18–21 June 2018; pp. 1–4. [CrossRef]

271. Fediuk, A.; Wilken, D.; Wunderlich, T.; Rabbel, W. Physical Parameters and Contrasts of Wooden Objects in Lacustrine Environment: Ground-Penetrating Radar and Geoelectrics. *Geosciences* **2020**, *10*, 146. [CrossRef]
272. Courville, S.W.; Putzig, N.E.; Sava, P.C.; Perry, M.R. Preparing to image the Martian subsurface: Planetary active-source seismology vs. radar, and the ARES concept. *AGU Fall Meet. Abstr.* **2019**, *2019*, P44B-05.
273. Lauro, S.E.; Mattei, E.; Cosciotti, B.; Di Paolo, F.; Arcone, S.A.; Viccaro, M.; Pettinelli, E. Electromagnetic signal penetration in a planetary soil simulant: Estimated attenuation rates using GPR and TDR in volcanic deposits on Mount Etna. *J. Geophys. Res. Planets* **2017**, *122*, 1392–1404. [CrossRef]
274. Pettinelli, E.; Burghignoli, P.; Pisani, A.R.; Ticconi, F.; Galli, A.; Vannaroni, G.; Bella, F. Electromagnetic Propagation of GPR Signals in Martian Subsurface Scenarios Including Material Losses and Scattering. *IEEE Trans. Geosci. Remote Sens.* **2007**, *45*, 1271–1281. [CrossRef]
275. Zhang, L.; Xu, Y.; Zeng, Z.; Li, J.; Zhang, D. Simulation of Martian Near-Surface Structure and Imaging of Future GPR Data From Mars. *IEEE Trans. Geosci. Remote Sens.* **2021**, *60*, 1–12. [CrossRef]
276. Thompson, T.W.; Campbell, B.A.; Ghent, R.R.; Hawke, B.R.; Leverington, D.W. Radar probing of planetary regoliths: An example from the northern rim of Imbrium basin. *J. Geophys. Res. Planets* **2006**, *111*, E06S14. [CrossRef]
277. Li, H.; Li, C.; Ran, S.; Feng, J.; Zuo, W. Applications of Surface Penetrating Radar for Mars Exploration. *AGU Fall Meet. Abstr.* **2015**, *2015*, P51C-2077.
278. Ip, W.-H.; Yan, J.; Li, C.-L.; Ouyang, Z.-Y. Preface: The Chang'e-3 lander and rover mission to the Moon. *Res. Astron. Astrophys.* **2014**, *14*, 1511–1513. [CrossRef]
279. Li, C.; Xing, S.; Lauro, S.E.; Su, Y.; Dai, S.; Feng, J.; Cosciotti, B.; Di Paolo, F.; Mattei, E.; Xiao, Y.; et al. Pitfalls in GPR Data Interpretation: False Reflectors Detected in Lunar Radar Cross Sections by Chang'e-3. *IEEE Trans. Geosci. Remote Sens.* **2017**, *56*, 1325–1335. [CrossRef]
280. Penasa, L.; Pozzobon, R.; Massironi, M.; Kang, Z.; Hu, T.; Rossi, A.P. 3D geologic model of the shallow subsurface of Chang'E 3 landing site (Sinus Iridum, Moon). In Proceedings of the 52nd Lunar and Planetary Science Conference, Online, 15–19 March 2021.
281. Fa, W.; Zhu, M.; Liu, T.; Plescia, J.B. Regolith stratigraphy at the Chang'E-3 landing site as seen by lunar penetrating radar. *Geophys. Res. Lett.* **2015**, *42*, 10,179–10,187. [CrossRef]
282. Li, C.; Zuo, W.; Wen, W.; Zeng, X.; Gao, X.; Liu, Y.; Fu, Q.; Zhang, Z.; Su, Y.; Ren, X.; et al. Overview of the Chang'e-4 Mission: Opening the Frontier of Scientific Exploration of the Lunar Far Side. *Space Sci. Rev.* **2021**, *217*, 35. [CrossRef]
283. Lai, J.; Cui, F.; Xu, Y.; Liu, C.; Zhang, L. Dielectric Properties of Lunar Materials at the Chang'e-4 Landing Site. *Remote Sens.* **2021**, *13*, 4056. [CrossRef]
284. Giannakis, I.; Zhou, F.; Warren, C.; Giannopoulos, A. Inferring the Shallow Layered Structure at the Chang'E-4 Landing Site: A Novel Interpretation Approach Using Lunar Penetrating Radar. *Geophys. Res. Lett.* **2021**, *48*, e2021GL092866. [CrossRef]
285. Dong, Z.; Fang, G.; Zhou, B.; Zhao, D.; Gao, Y.; Ji, Y. Properties of Lunar Regolith on the Moon's Farside Unveiled by Chang'E-4 Lunar Penetrating Radar. *J. Geophys. Res. Planets* **2021**, *126*, e2020JE006564. [CrossRef]
286. Li, C.; Su, Y.; Pettinelli, E.; Xing, S.; Ding, C.; Liu, J.; Ren, X.; Lauro, S.E.; Soldovieri, F.; Zeng, X.; et al. The Moon's farside shallow subsurface structure unveiled by Chang'E-4 Lunar Penetrating Radar. *Sci. Adv.* **2020**, *6*, eaay6898. [CrossRef] [PubMed]
287. Farley, K.A.; Schulte, M.D.; Williford, K.H. Overview of the Mars 2020 Mission and its Investigation Payload. In *International Workshop on Instrumentation for Planetary Missions*; NASA: Washington, DC, USA, 2014.
288. Mellon, M.T.; Sizemore, H.G. The history of ground ice at Jezero Crater Mars and other past, present, and future landing sites. *Icarus* **2021**, *371*, 114667. [CrossRef]
289. Hamran, S.-E.; Paige, D.A.; Amundsen, H.E.F.; Berger, T.; Brovoll, S.; Carter, L.; Damsgård, L.; Dypvik, H.; Eide, J.; Eide, S.; et al. Radar Imager for Mars' Subsurface Experiment—RIMFAX. *Space Sci. Rev.* **2020**, *216*, 128. [CrossRef]
290. Hamran, S.-E.; Berger, T.; Brovoll, S.; Damsgard, L.; Helleren, O.; Oyan, M.J.; Amundsen, H.E.; Carter, L.; Ghent, R.; Kohler, J.; et al. RIMFAX: A GPR for the Mars 2020 rover mission. In Proceedings of the 2015 8th International Workshop on Advanced Ground-Penetrating Radar (IWAGPR), Florence, Italy, 7–10 July 2015; pp. 1–4. [CrossRef]
291. Szymczyk, P. Classification of geological structure using Ground-Penetrating Radar and Laplace transform artificial neural networks. *Neurocomputing* **2015**, *148*, 354–362. [CrossRef]
292. Spanoudakis, N.S.; Vafidis, A.; Papavasiliou, A. Delineating a doline system using 3D Ground-Penetrating Radar (GPR) data, complex trace attributes and neural networks: A case study in Omalos Highlands, Hania, Crete. In Proceedings of the 1st International Conference on Advances in Mineral Resources Management and Environmental Geotechnology, Hania, Greece, 7–9 June 2004.
293. Campbell, S.W.; Briggs, M.; Roy, S.G.; Douglas, T.A.; Saari, S. Ground-penetrating radar, electromagnetic induction, terrain, and vegetation observations coupled with machine learning to map permafrost distribution at Twelvemile Lake, Alaska. *Permafr. Periglac. Process.* **2021**, *32*, 407–426. [CrossRef]
294. Qian, Y.; Forghani, M.; Lee, J.H.; Farthing, M.; Hesser, T.; Kitanidis, P.; Darve, E. Application of deep learning-based interpolation methods to nearshore bathymetry. *arXiv* **2011**, arXiv:2011.09707.
295. Ball, A.; O'Connor, L. Geologist in the Loop: A Hybrid Intelligence Model for Identifying Geological Boundaries from Augmented Ground-Penetrating Radar. *Geosciences* **2021**, *11*, 284. [CrossRef]

296. Sengani, F. The use of Ground-Penetrating Radar to distinguish between seismic and non-seismic hazards in hard rock mining. Tunn. Undergr. *Space Technol.* **2020**, *103*, 103470. [CrossRef]
297. Neal, A. Ground-Penetrating Radar and its use in sedimentology: Principles, problems and progress. *Earth-Sci. Rev.* **2004**, *66*, 261–330. [CrossRef]
298. Proulx-McInnis, S.; St-Hilaire, A.; Rousseau, A.N.; Jutras, S. A review of Ground-Penetrating Radar studies related to peatland stratigraphy with a case study on the determination of peat thickness in a northern boreal fen in Quebec, Canada. *Prog. Phys. Geogr. Earth Environ.* **2013**, *37*, 767–786. [CrossRef]
299. Ruffell, A.; Parker, R. Water penetrating radar. *J. Hydrol.* **2021**, *597*, 126300. [CrossRef]
300. Tatum, D.; Francke, J. Radar suitability in aeolian sand dunes A global review. In Proceedings of the 14th International Conference Ground-Penetrating Radar, Shanghai, China, 4–8 June 2012; pp. 695–700. [CrossRef]
301. Tosti, F.; Pajewski, L. Applications of radar systems in Planetary Sciences: An overview. In *Civil Engineering Applications of Ground-Penetrating Radar*; Springer: Cham, Switzerland, 2015; pp. 361–371.
302. Kannaujiya, S.; Chattoraj, S.L.; Jayalath, D.; Ray, P.K.C.; Bajaj, K.; Podali, S.; Bisht, M.P.S. Integration of satellite remote sensing and geophysical techniques (electrical resistivity tomography and Ground-Penetrating Radar) for landslide characterization at Kunjethi (Kalimath), Garhwal Himalaya, India. *Nat. Hazards* **2019**, *97*, 1191–1208. [CrossRef]
303. Jianliang, W.; Iqbal, I.; Sanxi, P.; Yang, Y.; Jie, L.; Tianyu, Z. Integrated Geophysical Survey in Defining Subsidence Features of Glauber's Salt Mine, Gansu Province in China. *Geotech. Geol. Eng.* **2021**, *40*, 325–334. [CrossRef]
304. Gaballah, M.; Alharbi, T. 3-D GPR visualization technique integrated with electric resistivity tomography for characterizing near-surface fractures and cavities in limestone. *J. Taibah Univ. Sci.* **2022**, *16*, 224–239. [CrossRef]
305. Zhao, W.; Forte, E.; Fontolan, G.; Pipan, M. Advanced GPR imaging of sedimentary features: Integrated attribute analysis applied to sand dunes. *Geophys. J. Int.* **2017**, *213*, 147–156. [CrossRef]
306. Farfour, M.; Economou, N.; Abdalla, O.; Al-Taj, M. Integration of Geophysical Methods for Doline Hazard Assessment: A Case Study from Northern Oman. *Geosciences* **2022**, *12*, 243. [CrossRef]
307. Saylam, K.; Averett, A.R.; Costard, L.; Wolaver, B.D.; Robertson, S. Multi-Sensor Approach to Improve Bathymetric Lidar Mapping of Semi-Arid Groundwater-Dependent Streams: Devils River, Texas. *Remote Sens.* **2020**, *12*, 2491. [CrossRef]
308. Kim, K.; Lee, J.; Ju, H.; Jung, J.Y.; Chae, N.; Chi, J.; Kwon, M.J.; Lee, B.Y.; Wagner, J.; Kim, J.-S. Time-lapse electrical resistivity tomography and Ground-Penetrating Radar mapping of the active layer of permafrost across a snow fence in Cambridge Bay, Nunavut Territory, Canada: Correlation interpretation using vegetation and meteorological data. *Geosci. J.* **2021**, *25*, 877–890. [CrossRef]
309. Corradini, E.; Eriksen, B.V.; Mortensen, M.F.; Nielsen, M.K.; Thorwart, M.; Krüger, S.; Wilken, D.; Pickartz, N.; Panning, D.; Rabbel, W. Investigating lake sediments and peat deposits with geophysical methods—A case study from a kettle hole at the Late Palaeolithic site of Tyrsted, Denmark. *Quat. Int.* **2020**, *558*, 89–106. [CrossRef]